4

Expression analysis of NLR gene family members in gliomas for identification of novel therapeutic interventions

4.1 ABSTRACT

Inflammation is an important hallmark of cancer. Chronic dysregulated inflammation may lead to DNA damage, mutations and epigenetic changes such as those seen in cancer. Gliomas are the most prevalent primary brain tumors with immense clinical heterogeneity and rapid invasion, making them refractory to treatment and, leading to poor prognosis and low survival [Louis, 2006; Furnari, Fenton *et al.*, 2007]. Understanding the role of causative genes that drive glioma growth and progression is essential for targeted therapeutics and prolonged survival of patients. Infiltrating immune cells form a major component of the tumor microenvironment [Charles, Holland *et al.*, 2012; Fathima Hurmath, Ramaswamy *et al.*, 2014]. NLRs and AIM2 are crucial for initiation, progression and promotion of several cancers[Janowski, Kolb *et al.*, 2013]; however, there are no reports linking NLRs and AIM2 to glioma pathology. Our aim was to investigate the regulation of NLR and AIM2 gene expression in glioma pathology (figure 4.1). First, we used a data-driven approach to identify NLRs and NLR-associated gene expression and methylation patterns in different grades of glioma, namely, high grade glioma: glioblastoma (GBM) and low grade gliomas (LGG). Strong inverse correlation for expression and methylation levels signifies the effective control of methylated CpG loci over gene expression in glioblastoma. The association of differentially expressed genes with patient survival highlights their prognostic significance in high and low grade gliomas. Genes including *Msr1*, *Nlrc4*, *Nlrp6, Casp1* and *Nod1* showed high significance with patient survival in low grade gliomas. Next, utilizing glioma and microglia cell lines we confirmed the role of the candidate prognostic protein NLRP12 in cell proliferation and colony formation. Our findings provide novel insights into differential regulation of NLRs and NLR-associated genes in LGG and GBM, and clinical importance of innate immune signaling pathways in glioma pathogenesis.

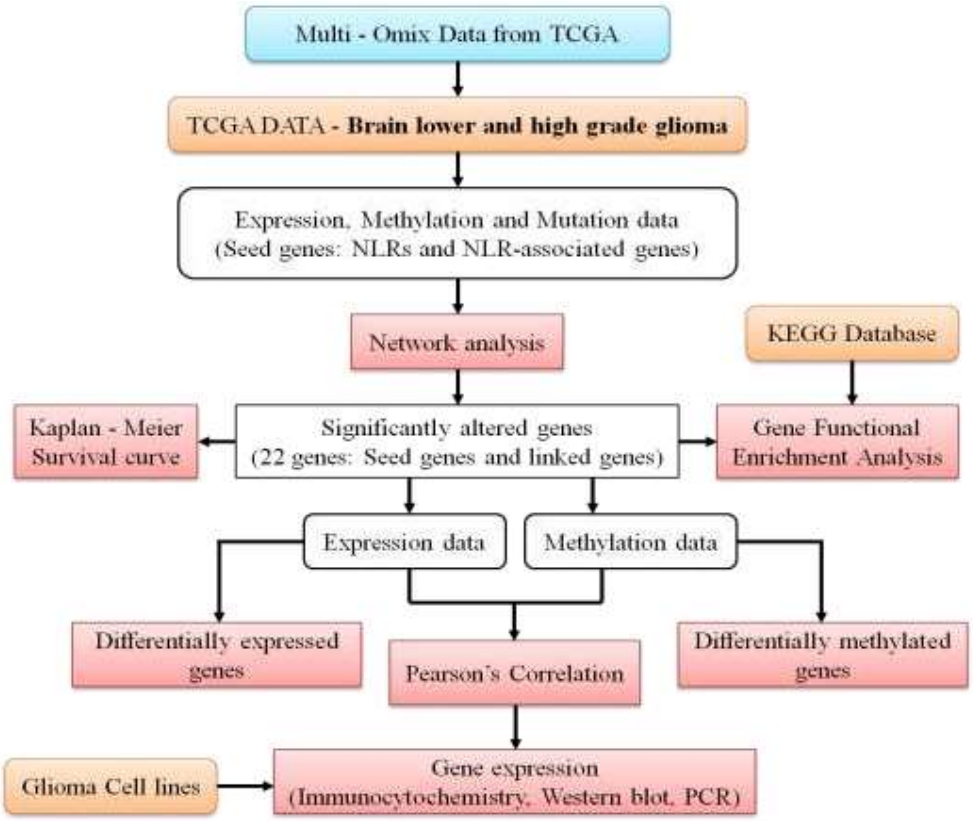

Figure 4.1: *Schematic flow diagram of multidimensional investigation exploring the role of specialized nucleotide-binding domain and leucine rich-repeat containing receptors (NLRs) in glioma pathology.*

4.2 INTRODUCTION

Gliomas are highly invasive and heterogeneous group of primary brain tumors with dismal prognosis of less than 15 months. Glioma accounts for 80% of primary malignant brain tumors[Schwartzbaum, Fisher *et al.*, 2006]. Depending on the degree of malignancy, gliomas have been classified into low and high grade glioma[Louis, Perry *et al.*, 2016]. LGG specifically represents 40% of all central nervous system (CNS) tumors in children[Sievert and Fisher, 2009]. While majority of high grade glioma occur *de novo*, it is common for approximately 70% of the well differentiated low grade glioma to progress into more aggressive form of glioma, GBM [Furnari, Fenton *et al.*, 2007]. As the name suggests, GBM is multiforme in every aspect; grossly (increased necrosis), microscopically (pleomorphic nuclei, microvascular proliferation) and genetically (gene deletion, mutation), with a median survival of less than 15 months [James and Olson, 1996; Stupp, Mason *et al.*, 2005]. GBM is rapidly lethal and forms 12–15% of all brain tumors and 50–60% of astrocytomas [Iacob and Dinca, 2009]. In spite of several multimodal treatment approaches (radiation, surgery and chemotherapy) and current therapeutic advances, glioma prognosis remains poor with high mortality rate [Stupp, Mason *et al.*, 2005]. Recent advances including cancer immunotherapy provide major treatment breakthroughs for a number of cancers [Mahoney, Rennert *et al.*, 2015; Gotwals, Cameron *et al.*, 2017] [Huang, Liu *et al.*, 2017]. Glioma cells are heavily infiltrated by the circulating innate immune cells, including majority of microglia and macrophages [Carvalho da Fonseca and Badie, 2013]. The cellular and molecular interactions between innate immune cells and glioma tissue, contributes to the highly

enriched microenvironment facilitating tumor growth and progression [Rivest, 2009; Yeh, Lu *et al.*, 2012]. Both immune and glioma cells communicate with each other by release of signaling molecules in order to promote tumor develoment [Hussain, Yang *et al.*, 2006].

Nucleotide-binding domain, leucine-rich repeat containing (NLR) proteins are cytoplasmic innate immune sensors; providing protection against foreign attacks, cellular damage and environmental stress [Ting, Lovering *et al.*, 2008]. NLRs sense several PAMPs and DAMPs such as nucleic acids, flagellin and glucose, extracellular ATP, UV radiation and other irritants [Davis, Wen *et al.*]. Hoffman *et al.* first identified association of a NLR family member, *NLRP3* dysfunction with a class of cryopyrin-associated periodic syndromes (CAPS) [Hoffman, Mueller *et al.*, 2001; Hoffman, Gregory *et al.*, 2003]. Today, dysregulation in NLR genes is associated with a wide array of diseases including major pathogen-induced infections, diabetes, cardiac and metabolic disorders, autoimmune diseases and cancers [Davis, Wen *et al.*, 2011; Freeman and Ting, 2016; Gharagozloo, Gris *et al.*, 2017]. Recent investigations define contrasting and cell-specific regulatory roles of NLRs, *NLRP3* and *NLRC4* in colorectal cancer both *in vitro* and *in vivo* [Allen, TeKippe *et al.*, 2010; Hu, Elinav *et al.*; Zaki, Boyd *et al.*]. Other NLRs, such as *NLRP6* and *NLRP12* serves as negative regulators of canonical *NF-κB* and *MAPK*-dependent inflammatory signaling for protection against colorectal cancer [Elinav, Strowig *et al.*; Allen, Wilson *et al.*, 2012; Chen]. NLRC3, a newly characterized NLR family member acts as a negative regulator for TLR-mediated signaling via modifications in adaptor, TRAF6 and transcription factor, NF-κB [Schneider, Zimmermann *et al.*, 2012; Gültekin, Eren *et al.*, 2014]. In addition, NLRC3 specifically mediates PI3K-mTOR inhibition to combat colon cancer [Karki, Man *et al.*, 2016]. I*n silico* studies have further demonstrated the promising role of NLRs in colorectal cancer using The Cancer Genome Atlas (TCGA) and other pan-cancer data platforms [Liu, Truax *et al.*, 2015]. An alarming increase in cancer incidence, clinical heterogeneity, largely affected young population and high patient loss present urgent need for effective glioma therapeutics.

Despite the critical role of NLR's in cancers, the physiological and functional significance of NLRs underlying the development and progression of gliomas remains largely unknown [Janowski, Kolb *et al.*, 2013]. The lack of knowledge regarding the innate immune mechanisms associated with glioma pathology spurred this study. Understanding the cellular and molecular basis of transition of well differentiated, low grade glioma towards high grade glioma is critical for identification, and development of novel therapeutic targets. Keeping this in mind, the current investigation is focused on providing basic insights into NLR and NLR-associated gene regulation in low and high grade glioma pathogenesis, using The Cancer Genome Atlas (TCGA) pan-cancer datasets. TCGA datasets fulfill the importance of a systematic approach, high sample numbers and genome alterations profiling. TCGA database comprises of large comprehensive molecular profiles and clinical outcome information coming from multiple sources and platforms [Cerami, Gao *et al.*, 2012; Tomczak, Czerwińska *et al.*, 2015]. Our study analyzes TCGA- LGG and GBM patient datasets to understand expression and methylation patterns of NLR and NLR-associated genes in glioma pathogenesis. Our findings demonstrate significant differential expression and methylation of NLRs in GBM as compared to the LGG. Further, *in silico* and *in vitro* analysis highlights progonostic importance of NLRs, as we observed significant association between NLR gene expression and glioma patient survival.

4.3 MATERIALS AND METHODS

4.3.1 Data extraction and sample selection

The glioblastoma (GBM) and low grade glioma (LGG) patient samples were selected from TCGA using the cBioPortal platform [Cerami, Gao *et al.*, 2012] [Gao, Aksoy *et al.*, 2013]. The mRNA (RNA seq V2 RSEM) and gene expression (TCGA, provisional) data was extracted and analyzed to obtain gene networks and heat maps. TCGA expression and methylation

experimental profiles were downloaded using the UCSC cancer browser [Fujita, Rhead *et al.*, 2010]. TCGA DNA methylation data, is generated using the Illumina Infinium Human Methylation- 450 platform and the RNAseq gene expression data (pancan normalized), is acquired by the IlluminaHiSeq.

4.3.2 Gene expression network analysis

Gene mRNA expression z-scores (RNA Seq V2 RSEM) profiling was used with z-score threshold of "± 2.0". The GBM and LGG networks were inclusive of genes with >10% alterations. The genetic alterations include mutations, copy number alterations and mRNA expression. The networks were simplified using Cytoscape, a network generating tool [Shannon, Markiel *et al.*, 2003]. The heat maps were constructed using the complete linkage clustering method and heatmap.2 function of R platform. The gene ontology and enrichment analysis was performed using ClueGO, a Cytoscape application [Bindea, Mlecnik *et al.*, 2009].

4.3.3 Expression and methylation analysis

Gene expression and methylation data profiling was performed using R version 3.3.2. The differentially expressed genes and methylated CpG loci regions were identified using limma and minfi, R packages [Smyth, 2005; Aryee, Jaffe *et al.*, 2014]. Kaplan-Meier survival analysis was used to estimate the survival distributions in the gene expression dataset of TCGA glioma patients. The survival curves were generated to visualize the association between the expression of gene of interest and patient survival.

4.3.4 Cell Culture

A172 and LN-18, human glioblastoma cell lines were obtained from ATCC (ATCC® CRL-1620™, CRL-2610™). RAW264.7 (murine macrophages), C6 (rat glioma), CHO (Chinese hamster ovary), A549 (human lung alveolar epithelial cells) and HEK293T (Human embryonic kidney fibroblasts) cells were purchased from cell culture repository of National Centre of Cell Science (NCCS), Pune, Maharashtra, India. N9 and BV-2, immortalized murine microglial cells were a kind gift from Dr. Anirban Basu, National Brain Research Centre, Gurgaon, Delhi, India. Cells were grown on Dulbecco's modified eagle medium (DMEM), (Himedia, AL007S) with 10% Fetal bovine serum (Himedia, RM10432) and 1% antibiotic antimycotic solution (Sigma-Aldrich, A5955). Cell lines were cultured as per company instructions in humidified CO_2 incubators.

4.3.5 Bradford assay for protein estimation

For protein extraction, 0.25×10^6 cells were lysed using 0.25 ml RIPA buffer, in the presence of protease inhibitor (S8820 Sigma) and incubated for 5 minutes at room temperature followed by centrifugation at 13,000 rpm for 20 minutes, as described previously [Mariathasan, Newton *et al.*, 2004]. The supernatants were used for further analyses. Protein concentrations were determined using a coomassie (Bradford) protein assay kit and Nanodrop Spectrophotometer by taking absorbance measured at 595nm.

4.3.6 Fluorescence Microscopy

For immunofluorescence, we seeded $5x10^4$ cells per well of a 2-well chamber slide and incubated overnight. To simulate inflammation, cells were pre-stimulated with LPS (0.5 µg/mL; Sigma, L4391) for 12 hours. The cell culture media was discarded from the wells and cells were washed thrice with 1X PBS (Molecular biology grade, Himedia) for 3 minutes each. Cells were fixed with 4% PFA (MB Grade, Himedia) for 10 minutes and washed thrice with 1X PBS for 3 min each. The fixed cells were permeabilized with 0.1% TritionX-100 (Molecular biology grade, Sigma) in 1X PBS for 15 minutes. To avoid non-specific binding, blocking was performed with 5% Fetal Boveine Serum (Sterile filtered, Himedia) in 0.1% TritonX-100-PBS for 1 hour at 4^0C. Cells were immunolabeled by primary antibody incubation for overnight at 4^0C. The primary antibodies were used in following dilutions – anti-ASC (1:250), anti-AIM2 (1:200), anti-CASP1 (1:100) and anti-NLRP12 (1:300). Cells were washed 5 times with 1X PBS for 5 minutes each.

Followed by, secondary antibody incubation for 1 hour at room temperature (in dark). Next, cells were washed 5 times for 5 minutes each with 1X PBS. Nuclei were stained with 4',6-diamidino-2-phenylindole (DAPI, Sigma). Immunofluorescence was observed using fluorescence microscope (Leica Systems) and analyzed using ImageJ software [Schneider, Rasband *et al.*, 2012].

4.3.7 Colony formation assay

The cells were seeded at a cell density of 40 cells per well in a 2-well chamber slide and allowed to grow in an incubator (5% CO_2; 37°C). We observed few small colonies formed on third day. We added 50/100 nM scrambled (Dharmacon) and NLRP12 (Genetex) siRNA as suggested by the company protocol. The siRNA containing medium was removed after 6 hours and cells were incubated in fresh medium for next 24-48 hours. After media removal, cells were washed with 1X PBS for 2-3 minutes and stained with Giemsa (Himedia) for 20 minutes. The stain solution was discarded, and slides were washed gently with distilled water and air-dried. We then took slides for bright field imaging and captured images using the cell phone camera. For colony formation quantification, we performed number of colonies formed per well and cell count per colony.

4.3.8 Cell proliferation assay

The effect of *AIM2* and *NLRP12* inhibition on cell proliferative capacity was assessed using the MTT assay. We performed rapid 96-well plate transfections by preparing complexes in the plate and plating cells (10^3 cells per well) directly into the transfection mix. The siRNA containing media was replaced with 100µl of fresh DMEM complete media after 6-8 hours and incubated cells for 24 hours at 37ºC in a CO2 incubator (Model-170S, Eppendorf). For assay, we added 100µl of fresh DMEM complete media and 10µl of MTT (3-(4,5-Dimethylthiazol-2-Yl)-2,5-Diphenyltetrazolium Bromide) solution (M2128, Sigma) was added to each well. The plate was kept in incubator for 3 hours. After incubation, 100µl of acid/alcohol solution was added to each well. Absorbance was measured at 570nm using multi-mode microplate reader (Synergy H1 Hybrid, Biotek Instruments Inc).

4.3.8 Statistics

The student's T-test was performed and p-values below 0.05 (*p-value <0.05; **p-value <0.005) were considered statistically significant. For analysis, the Pearson's correlation coefficient was calculated to identify significant correlation between the gene expression and methylation data of TCGA glioma patient datasets.

4.4 Results and Discussion

4.4.1 Visualising NLR gene expression pattern in gliomas using microarray analysis

We analyzed the expression of the 22 NLR gene family members and their associated signaling components in LGG and GBM. Microarray gene expression data for LGG and GBM was obtained from the TCGA database using cBioPortal, a platform for cancer genomics data download, visualization and analysis. The mRNA expression (RNA seq V2 RSEM) z-scores profiling data comprised of LGG (527 samples) and GBM (166 samples) tumor samples, with a z-score threshold of "± 2.0". Microarray analysis of NLR gene expression in LGG and GBM was performed by generating clustered heat maps, using CIMminer, a bioinformatics tool [Weinstein, Myers *et al.*, 1997]. The expression analysis revealed differential expression of NLR genes across the GBM and LGG tumor samples (Figure 4.2-4.3). Interestingly, *Nod1* shows increased expression for almost all GBM samples. *Nlrp1, Nod2, CIITA, Nlrc4* and *Nlrp3* genes are up-regulated and down-regulated in almost half of the patient samples respectively. *Nlrp2, Nlrp7* and *Nlrp4* genes are down-regulated in most of the LGG samples. On contrary, *Nlrp11*

expression is up-regulated throughout the LGG samples. However, the *Nlrp5, Nlrp10* and *Nlrp13* gene expression remained unchanged in both low and high grade glioma.

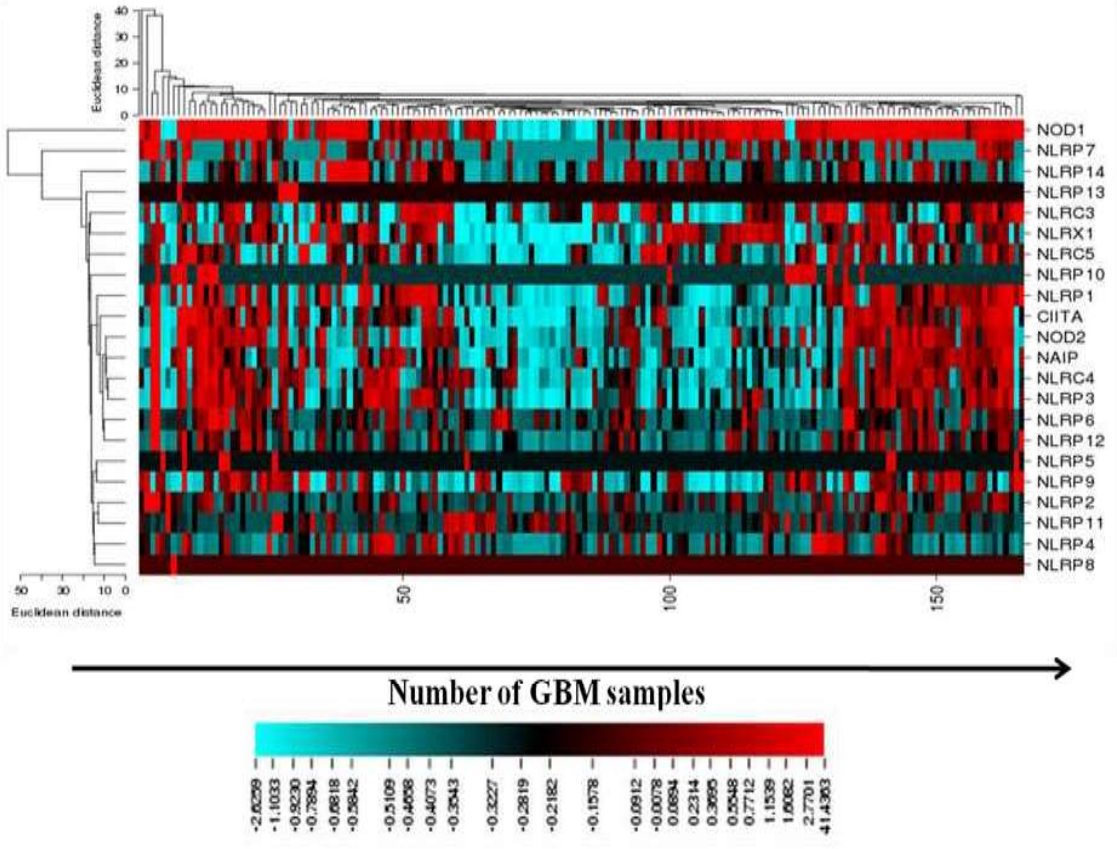

Figure 4.2 : *NLR gene expression pattern in glioblastoma using TCGA database.* Microarray expression data for GBM was obtained from the TCGA database. Expression (RNA seq V2 RSEM) data comprising of GBM (166 samples) tumor samples was used. The mRNA expression profiling was performed with a threshold of "± 2.0". A CIMminer-generated heat map was created for the expression data. Here, low expression is compared to the mean value which is a negative number and is colored blue whereas, high expression is denoted positive and colored red. The color coding is shown in the color bar.

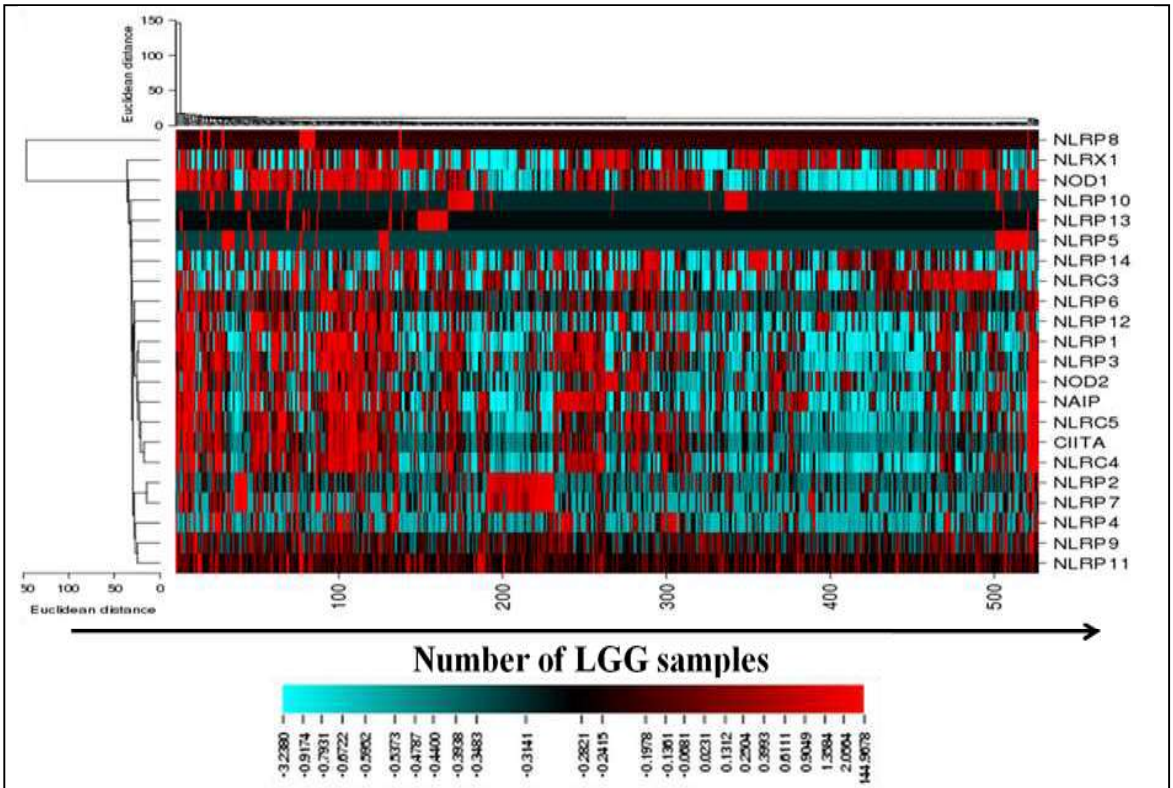

Figure 4.3 : *NLR gene expression pattern in low grade glioma using TCGA database.* Microarray expression data for LGG was obtained from the TCGA database. Expression (RNA seq V2 RSEM) data comprising of LGG samples (527 samples) was used. The mRNA expression profiling was done with z-score threshold of "± 2.0". A CIMminer-generated heat map was created for the expression data. Low expression is compared to the mean value which is a negative number and is colored blue whereas, high expression is denoted positive and colored red. The color coding is shown in the color bar.

4.4.2 Network analysis of NLR gene expression in low grade glioma and glioblastoma

The cellular and molecular complexity of glioma and cross-talk within the tumor microenvironment brings into focus the dysregulated genomic and epigenetic variations occurring in glioma. We need to understand the genomic signature underlying the generation of LGG, GBM and sometimes, progression of LGG into GBM. NLRs, are innate immune receptors that perform multiple regulatory functions in major inflammation-associated pathways, such as NF-κB, MAPK regulation as well as anti-inflammatory signaling to maintain immune surveillance [Zanotto-Filho, Gonçalves *et al.*, 2017]. As discussed already, NLRs play both tumor-promoting and –inhibitory roles in cancers [Kent and Blander, 2014]. However, the function and regulation of NLRs in glioma pathogenesis remains unidentified. Therefore, to understand the importance of NLRs and their interactions in glioma, LGG and GBM patient datasets were extracted from the TCGA database [McLendon, Friedman *et al.*, 2008]. We first generated glioma networks using the cBioPortal cancer genomics platform [Cerami, Gao *et al.*, 2012; Gao, Aksoy *et al.*, 2013]. The networks were then simplified using Cytoscape, an open source software for integrating biomolecular interaction networks with high-throughput expression data into a unified conceptual framework [Shannon, Markiel *et al.*, 2003]. The **seed genes** (genes of interest) included *NLRP3, NLRP6, NLRP12, NLRC3, NLRC4, NLRX1, PYCARD, CASP-1, AIM2, MSR1* and *NOD2*. The pathway was found to be altered in 38.9% cases for LGG and in 38.5% cases for GBM (Figure 4.4). Along with our seed genes, the networks also included other genes that we named as **linked genes**. Collectively, we termed all these genes as our **network genes**. Most frequently altered genes in LGG were *TP53* (54% altered); and *EGFR* and

CDK11B (15 to 20% altered); and *AIM2*, *NLRP6*, *CASP1*, *NLRP3*, *NLRC4*, *NLRP12*, *CARD8*, *BCL10*, *ATN1*, *NLRX1* and *MAVS* (5 to 10% altered). Genes such as *MSR1*, *NOD2*, *PYCARD* and *NLRC3* were altered in less than 5% of LGGs. Notably, *TP53* (53% mutated) and *EGFR* (6% mutated) were the most frequently mutated driver genes across LGG.

The GBM network shows *EGFR* (65% altered), *NOD1* (40% altered) and *TP53* (35% altered) as most frequently altered genes (Figure 4.4). Other frequently altered genes were *MAVS* (15% altered) and *PSEN1* (23% altered); and *CARD8*, *PARP1* and *BCL2L1* (10-15% altered); *MAVS*, *NLRC3*, *NLRX1, NLRP6*, *PYACRD*, *CASP1*, *NLRP3*, *NLRP12* and *NOD2* (5-10% altered). Genes including *AIM2* and *NLRC4* were altered in less than 5% of GBMs. As expected, *EGFR* (32.6% mutated) and *TP53* (31.9% mutated) emerged as the highly mutated driver genes for GBMs. Interestingly, *TP53* was more frequently altered and mutated in LGG as compared to the GBM. Similarly, *EGFR* was more frequently altered and mutated in GBM as compared to the LGG (Figure 4.4). Several genomic alterations in *EGFR* and *TP53* are known to contribute significantly in tumors, including glioma [Herbst, 2004; Olivier, Hollstein *et al.*, 2010]. Most of the linked genes, emerged through network analysis have important functional roles associated with DNA damage repair, cell proliferation, cell death, tumor-suppressor and other core cell signaling pathways [Ushio, Tada *et al.*, 2003; Bruey, Bruey-Sedano *et al.*, 2007; Underhill, Toulmonde *et al.*, 2010; Kim, Rait *et al.*, 2014; Ismail, Dronyk *et al.*, 2016; Zhang, Zhang *et al.*, 2016]. Thus, the glioma networks reflect possibility of significant regulatory expression and signaling of NLRs and other-associated genes in glioma pathogenesis.

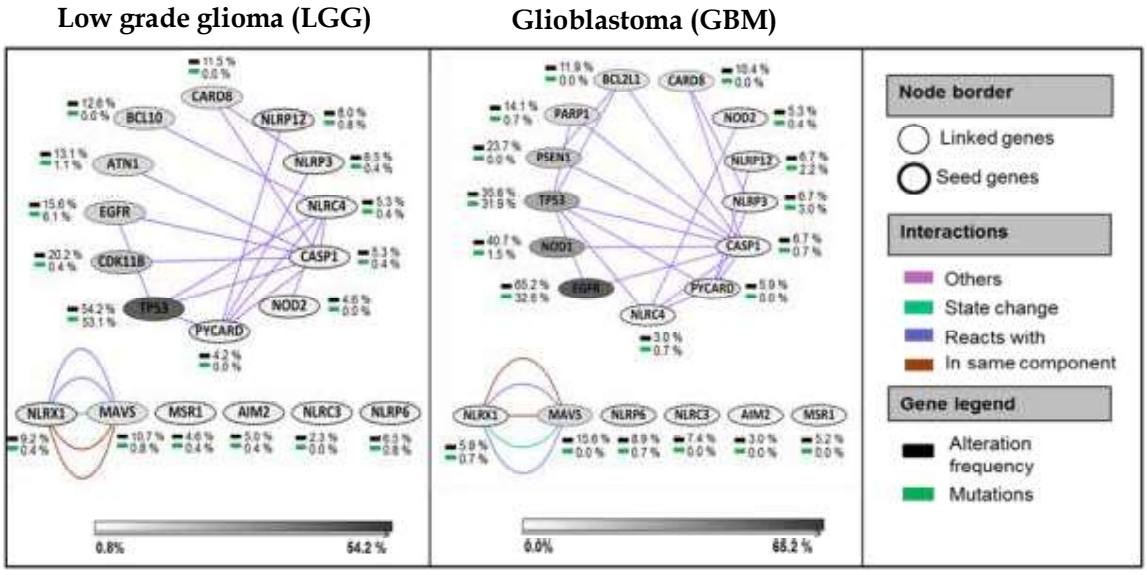

Figure 4.4 : *NLR gene expression networks in low grade glioma and glioblastoma.* Networks for LGG and GBM were generated using the TCGA database from the cBioPortal platform for cancer genomics. The network generation was restricted to genes with alteration greater than 10%. Glioma pathways were found to be altered for 38.9% and 38.5% of LGG and GBM cases respectively. Node border, interactions and gene legends are specified in the key on the right.

4.4.3 Differential expression of NLRs and NLR-associated regulatory components in LGG and GBM

The World Health Organization (WHO) has classified glioma into four grades, depending on the degree of malignancy [Louis, Perry *et al.*, 2016]. On the basis of histology, the LGG is stratified into grade 2 and grade 3 glioma. The grade 2 and 3 glioma, are further divided into three histological types – astrocytoma, oligoastrocytoma, and oligodendroglioma. Grade 4 glioma is a highly aggressive advanced form of glioma, well known as glioblastoma (GBM). However, there is no clear distinction between different grades of glioma, based on their histology. Cancer results from genomic alterations, including copy number variation, mutation and methylation [Ohgaki and Kleihues, 2009; Project, 2013]. Genes (seed and linked genes) obtained through network analysis were investigated further using quantitative genomic analysis. The gene expression analysis provides mechanistic insight into the associated pathways undergoing alterations across different grades of glioma. We first studied the expression of seed and linked genes, including NLRs using heat map representation (Figure 4.5). We generated heat map to visualize the relative gene expression, between grade 2 and 3 of LGG. We could see overlapping gene expression profiling of samples for grade 2 and 3 of LGG (Figure 4.5(a)). Next, we performed a comparative analysis of GBM (grade 4) and LGG by generating heat maps for, grade 4 vs. grade 2 and grade 4 vs. grade 3 gliomas. Interestingly, we observed characteristic gene expression pattern for GBM as compared to both grade 2 and 3 LGG (Figure 4.5(b, c)). The heat maps highlight overlapping expression profiling for LGG samples, but distinct gene expression clusters for GBM as compared to the LGG.

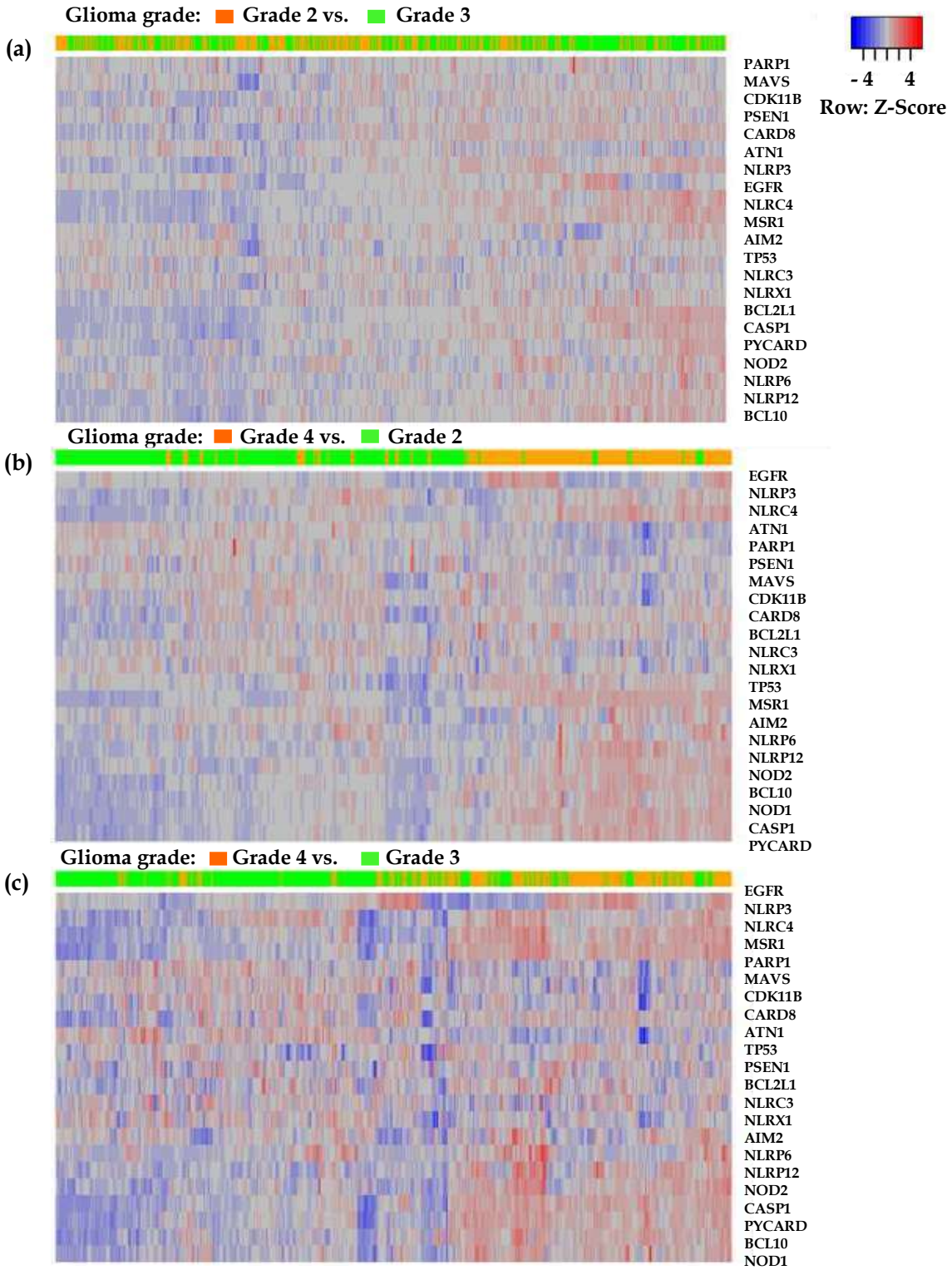

Figure 4.5 : *Heat map clustering for NLR gene expression in glioma.* (a) Shows NLR gene expression across grade 2 (orange) - grade 3 (green) of LGG samples. (b, c) Shows NLR gene expression between grade 4 (GBM, orange) – grade 2 (LGG, green) and grade 4 (GBM, orange) – grade 3 (LGG, green) glioma samples respectively. Each row represents specific gene expression across the tumor samples, represented in columns. Here, relative up-regulated gene expression is shown in red, while down-regulated gene expression is shown in blue.

To further understand the pattern of NLR gene expression in LGG and GBM, we performed differential gene expression analysis across different grades of glioma; grade 3 vs. grade 2, grade 4 vs. grade 2 and grade 4 vs. grade 3 (Table 4.1). The RNAseqV2 (Illumina HiSeq platform, pan-can normalized) microarray datasets for LGG and GBM were analyzed for the network genes (seed and linked genes) across all TCGA cohorts. Differential gene expression was calculated in terms of $\log_2$ fold change and adjusted p- values (Table 4.1). We noticed that NLRs and other associated genes did not have significant differential gene expression across the grade 2 and grade 3 of LGG (shown in Table 4.1). The differential gene expression analysis between LGG provided significantly low $\log_2$ fold change values. However, we observed significant differential gene expression for network genes in GBM with respect to the grade 2 and 3 of LGG. Genes, such as *MSR1, NOD2, NLRP12, NLRC4, PYCARD and CASP1* showed most significantly differentially expressed genes ($\log_2$ fold change - greater than or equal to 1) in GBM with respect to LGG. In fact, in line with the presence of macrophages in glioma, we saw increased MSR1 expression. MSR1 (Macrophage scavenger receptor-1) is associated with endocytosis of LDLs (low density lipids). MSR1 ranked first amongst most differentially expressed genes in GBM, with high fold change (positive) value with respect to LGG. In network analysis, *TP53* was one of most frequently altered gene across LGG and GBM. *TP53* also emerged as highly differentially expressed gene in GBM as compared to LGG. Notably, *NLRP12* and *NOD2* show significantly low expression levels in GBM as compared to the LGG (Table 4.1).

The data resulting from the differential gene expression analysis provides novel view of altered innate immune signaling and other core cell signaling pathways in glioma pathogenesis. The increased expression of *MSR1, TP53, NOD1, NLRC4, EGFR* and *MAVS* genes in GBM (Table 4.1), shows increased possibility of these genes being involved in signaling pathways active in glioma regulation. Genetic alterations in *TP53* and *EGFR* in cancers have been very well researched so far. *EGFR* overactivation in GBM, leads to subsequent activation of multiple downstream signaling pathways such as phosphatidylinositol 3-kinase (PI3K)/Akt/rapamycin-sensitive mTOR-complex (mTOR) pathway, followed by poor prognosis and drug resistance [Li, Wu *et al.*, 2016]. Similarly, *NOD1* activation promotes cancer cell growth and metastatic potential in colon cancer [Couturier-Maillard, Secher *et al.*, 2013]. *TP53*, a very well studied tumor suppressor gene creates a complex signaling network by contributing to major signaling pathways associated with cell cycle, DNA repair, apoptosis, angiogenesis and metabolism, and others [Lane and Levine, 2010; Olivier, Hollstein *et al.*, 2010]. As a result of major genetic alterations, *TP53* is one of the key driver genes in LGG and GBM. MSR1 is macrophage-specific integral membrane glycoprotein, implicated in various macrophage-associated physiological and pathological processes including phagocytosis, colon cancer, ovarian cancer and host defense [Miller, Zheng *et al.*, 2003; Mathioudaki, Leotsakou *et al.*, 2004; Taylor, Martinez-Pomares *et al.*, 2005; Leoutsakou, Talieri *et al.*, 2006]. *MSR1* expression has been reported in high grade gliomas, and glioma cells positively regulate *MSR1* expression in macrophages [Zhang, Zhang *et al.*, 2016]. Importantly, tumor-associated macrophages gene signature, comprising of distinct M2-macrophage related gene - *MSR1*, are highly enriched in GBM tumors.

Table 4.1 : *Differential gene expression of NLRs in low grade glioma (LGG) versus glioblastoma (GBM)*

Between groups	**Grade 3 vs. Grade 2**		**Grade 4 vs. Grade 2**		**Grade 4 vs. Grade 3**	
Gene	**log_2FC**	**Adjusted p-value**	**log_2FC**	**Adjusted p-value**	**log_2FC**	**Adjusted p-value**
MSR1	**0.79**	4.97E-07	**3.00**	8.41E-69	**2.22**	2.09E-39
TP53	0.37	9.35E-06	0.76	1.07E-17	0.39	1.54E-06
BCL10	0.19	6.29E-05	0.82	1.00E-57	0.63	3.33E-35
CASP1	**0.48**	1.48E-04	**1.70**	2.03E-40	**1.23**	7.32E-20
NOD1	0.26	3.02E-04	0.70	1.34E-18	0.43	9.23E-08
NLRC4	**0.27**	1.01E-02	**0.95**	1.28E-20	**0.68**	2.77E-10
CARD8	0.16	1.01E-02	0.30	3.50E-07	0.14	1.73E-02
EGFR	0.45	1.01E-02	0.87	1.22E-05	0.41	7.10E-02
PSEN1	-0.11	1.01E-02	-0.13	2.38E-03	-0.02	6.90E-01
MAVS	0.09	1.01E-02	-0.16	4.30E-04	-0.26	6.16E-10
NLRP12	**0.22**	1.76E-02	**1.16**	8.98E-23	**0.94**	9.18E-16
PYCARD	**0.26**	2.68E-02	**1.32**	3.18E-29	**1.06**	1.21E-19
NOD2	**0.21**	6.57E-02	**1.03**	3.27E-16	**0.82**	2.62E-11
ATN1	-0.07	1.20E-01	-0.67	3.92E-34	-0.60	2.79E-28
NLRP6	0.17	1.20E-01	0.16	1.67E-01	-0.01	8.98E-01
CDK11B	0.05	2.53E-01	-0.16	4.30E-04	-0.21	2.11E-06
BCL2L1	0.04	4.36E-01	0.18	8.77E-05	0.14	3.57E-03
PARP1	0.02	5.46E-01	-0.23	2.61E-08	-0.26	1.10E-11
NLRC3	-0.03	5.69E-01	-0.32	7.34E-09	-0.29	3.38E-07
AIM2	-0.05	6.89E-01	-0.13	3.31E-01	-0.08	6.15E-01
NLRX1	-0.02	7.48E-01	-0.38	1.14E-12	-0.37	5.35E-11
NLRP3	-0.03	8.08E-01	-0.10	3.50E-01	-0.07	6.15E-01

*****_NLRs and NLR-associated genes are differentially expressed in glioma._ The first column lists NLRs and other linked genes, showing differential expression across different glioma grades; low grade glioma (column 2) and glioblastoma (column 3 and 4). log_2FC represents log fold change (FC). Here, p-value <0.05 is significant.

4.4.4 Methylation of NLRs and NLR-associated genes in glioma

Methylation, an epigenetic modification holds significant control over gene transcription for stable regulation of gene expression. The reversible nature of methylation makes it a promising therapeutic approach for effective gene regulation and tumor suppression [Bird, 1986]. Targeting DNA methylation of specific biomarker gene promoter regions such as *MGMT* methylation has undoubtedly favored glioma prognosis and improved survival [Dunn, Baborie *et al.*, 2009]. Keeping in mind, the genome-wide importance of methylation, we looked at the methylation levels of CpG loci in network genes (seed genes and linked genes) for LGG and GBM using TCGA- GBM and LGG patient datasets. We have identified significant differential methylation of CpG loci corresponding to the network genes using R packages. Table 4.2 shows differentially methylated CpG loci for specific gene expression, comparing GBM and LGG glioma grades, grade 4 vs. grade 2 and grade 4 vs. grade 3 respectively. The influence of methylation over expression was calculated using the Pearson's correlation coefficient between gene expression and methylation levels. Notably, we observed highly significant negative correlation between gene expression and methylation levels for most of the network genes, in case of GBM (Table 4.2).

TP53, a tumor suppressor gene is highly altered in GBM and *TP53* association with poor prognosis and overall survival of GBM patients, making it a potential therapeutic target [Kim, Rait *et al.*, 2014]. Despite of higher fold change expression of *TP53* gene in GBM as compared to LGG, we did not find any significant correlation between *TP53* methylation and expression in GBM (Table 4.2). Probably, here methylation does not have significant control over silencing of *TP53* transcription and expression, raising possible involvement of other epigenetic mechanisms associated with genes involved in the *TP53* pathway.

Several studies have proved methylation-associated *PYCARD* silencing across multiple cancer types. Stone *et al.*, first identified aberrant methylation of CpG Island in the *PYCARD* promoter region methylation, resulting in reduced or complete loss of PYCARD expression in human glioblastoma cell lines. *PYCARD*, also known as apoptosis-associated speck-like protein containing CARD (*ASC*) is involved in several cell death-associated pathways [Stone, Bobo *et al.*, 2004]. ASC/*PYCARD* also mediates inflammasome formation upon activation through various sterile, environment-derived and cellular damage associated stimuli [Davis, Wen *et al.*]. Our findings confirm high inverse correlation between *PYCARD* expression and methylation levels in case of glioblastoma.

We found differential expression and significantly methylated CpG loci for *NLRP3* (cg21991396, cg07313373) and *CASP1* (cg21002651, cg13802966) in GBM. Recently published research from Paugh *et al.*, shows significantly higher expression of CASP1 and its activator *NLRP3* in glucocorticoid resistant leukemia cells, due to significantly low somatic methylation of *CASP1*(cg13802966) and *NLRP3* (cg21991396) promoters [Paugh, Bonten *et al.*, 2015]. The authors have also elucidated a novel mechanism by which NLRP3/CASP1 inflammasome modulates cellular levels of the glucocorticoid receptor and makes leukemia cell sensitive to glucocorticoids [Paugh, Bonten *et al.*, 2015]. Interestingly, we also found significant inverse correlation between methylated CpG loci and expression in GBM, for genes - *AIM2*, *ATN1*, *BCL2L1*, *CASP1*, *EGFR*, *MSR1*, *NLRC3*, *NLRC4*, *NLRP3*, *NLRP12*, *NLRX1*, *NOD1*, *NOD2*, *PYCARD*, *CDK11B* and *PSEN1*(Table 4.2). Highly significant inverse correlation of gene expression and methylation for some differentially expressed genes is also depicted through box-plots (Figure 4.6).

Table 4.2: *Differentially methylated genes in low grade glioma (LGG) and glioblastoma (GBM)*

		Grade 4 vs. Grade 2		Grade 4 vs. Grade 3			Grade 4	
Gene	**CpG loci**	**log_2FC**	**adjusted p-value**	**log_2FC**	**adjusted p-value**	**Dist. from TSS**	**Corr. coeff. (ρ)**	**p-value**
AIM2	cg11003133	-0.23	3.96E-56	-0.25	6.88E-64	256	-0.26	4.42E-02
	cg00490406	-0.09	2.29E-25	-0.09	1.92E-27	-126	-0.34	6.52E-03
ATN1	cg09215316	0	1.36E-02	-[A]	-	3	-0.24	5.90E-02
	cg11831988	-	-	0	1.48E-01	53	-0.36	3.74E-03
BCL2L1	cg08619561	0	7.40E-07	-	-	47	-0.24	6.12E-02
	cg02457826	-	-	0	4.10E-02	-77	-0.27	3.05E-02
BCL10	cg06913958	-0.33	3.15E-53	-0.33	3.82E-57	-2054	-0.43	4.76E-04
CASP1	cg21002651	-0.32	5.56E-47	-0.35	3.20E-56	-49	-0.68	1.49E-09
	cg13802966	-0.2	1.28E-42	-0.24	6.10E-58	6	-0.39	1.94E-03
EGFR	cg18809076	-0.25	2.35E-23	-0.32	8.60E-37		-0.76	1.21E-12
	cg14344486	-0.06	1.91E-18	-0.07	2.96E-22	-25141	-0.81	1.38E-15
MSR1	cg16303562	-0.19	2.36E-36	-0.2	3.81E-39	-33	-0.25	5.12E-02
NLRC3	cg00011564	-0.04	1.70E-12	-0.04	1.76E-14	-7473	-0.28	2.66E-02
	cg04082551	-0.04	6.82E-08	-0.04	1.39E-08	-7605	-0.28	3.05E-02
NLRC4	cg22805603	-0.12	1.35E-29	-0.12	4.41E-34	46	-0.45	2.67E-04
	cg07055315	-0.19	2.27E-17	-0.22	2.38E-24	-23	-0.26	4.45E-02
NLRP3	cg07313373	-0.23	2.55E-43	-0.25	2.52E-49	-326	-0.36	4.15E-03
	cg21991396	-0.11	1.47E-23	-0.12	2.14E-25	63	-0.35	5.64E-03
NLRP12	cg07042144	-0.1	9.73E-23	-0.11	4.23E-26	244	-0.6	2.62E-07
	cg22337438	-0.08	6.47E-13	-0.08	3.46E-14	211	-0.66	4.55E-09
NLRX1	cg26863308	-0.14	3.99E-10	-0.18	6.10E-16	611	-0.44	3.17E-04
	cg24516766	-	-	0	1.68E-01	-	-0.57	1.56E-06
NOD1	cg04071779	-0.35	4.10E-48	-0.38	4.23E-59	766	-0.35	5.61E-03
	cg09579281	-0.07	9.46E-17	-0.08	1.16E-23	3107	-0.32	1.05E-02
NOD2	cg16771652	-0.1	1.81E-22	-0.1	1.02E-26	-664	-0.6	2.70E-07
	cg04172533	-0.06	7.52E-12	-0.07	1.11E-13	-1441	-0.68	1.39E-09
PYCARD	cg05907835	-0.11	5.31E-17	-0.11	1.10E-17	-249	-0.54	6.28E-06
	cg12100791	-0.06	1.30E-10	-0.06	3.08E-12	-320	-0.56	1.93E-06
CDK11B	cg21921584	-0.03	1.00E-05	-0.04	4.81E-08	3891	-0.35	5.23E-03
	cg09283376	0.01	3.04E-03	0.02	5.56E-05	-	-0.43	4.83E-04
PSEN1	cg13173405	-0.01	9.07E-02			-191	-0.39	1.61E-03
	cg26376566	-	-	0	5.11E-02	-	-0.38	2.36E-03

*****_Significantly differentially methylated CpG loci for NLRs and NLR-associated genes._ Here, the table shows genes with their differentially methylated CpG loci in LGG and GBM. We calculated correlation coefficients and their value of significance of NLRs and other linked genes in case of glioblastoma. log fold change is represented as log_2FC. Here, p-value <0.05 is significant. Distance from transcription start site is abbreviated as Dist. from TSS. Correlation coefficient (Corr. coeff.) abbreviated as ρ. [A]Dash denotes CpG loci not being significant for that grade.

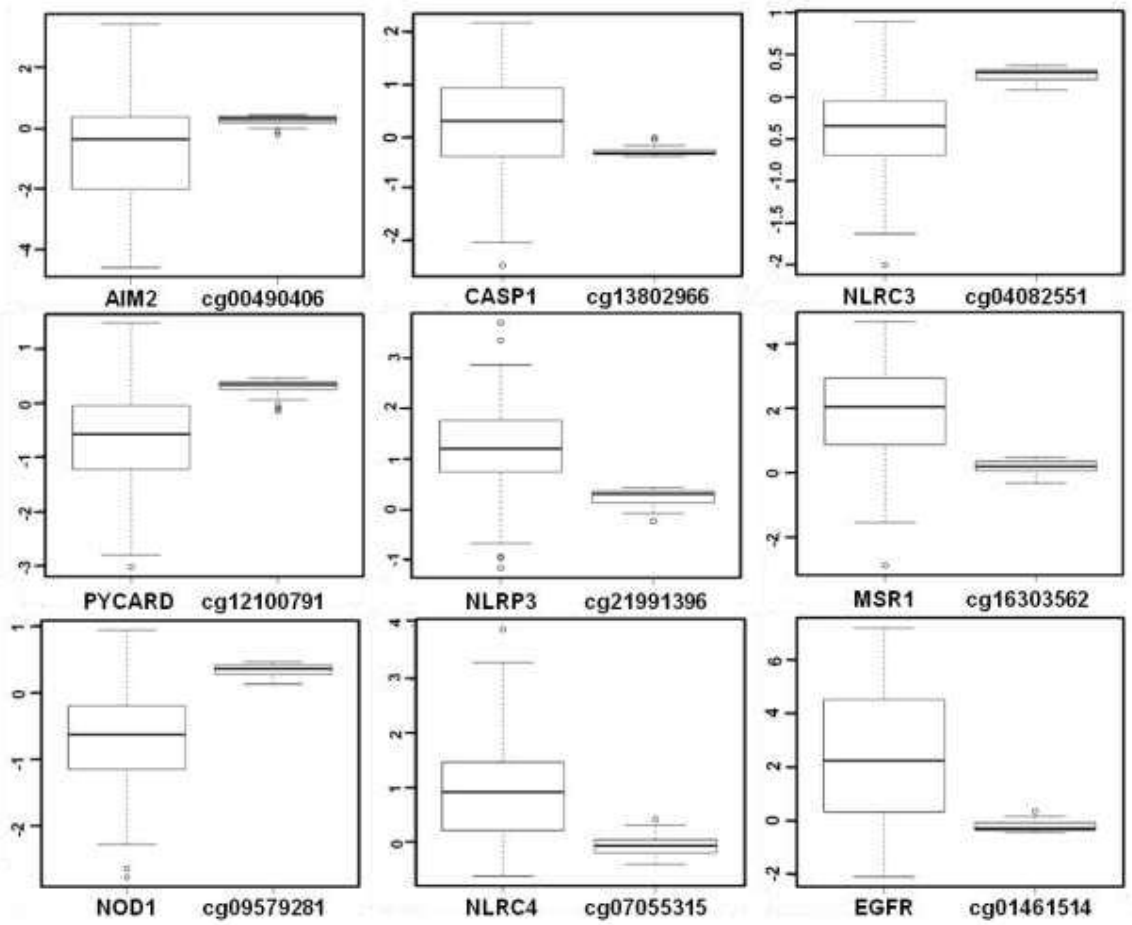

Figure 4.6 : *Negative regulation of NLR gene expression by methylation in glioblastoma*. The box plots show significant inverse correlation between expression of NLRs and NLR-associated genes and differential methylation levels. Pearson's correlation coefficient - p-value <0.05.

4.4.5 Gene ontology analysis

To develop a better understanding of the cellular and molecular interactions between highly altered genes in glioma, gene enrichment analysis (GEA) was performed using available data and knowledge bases. The gene ontology (GO) analysis was carried out using publicly available collection of gene functions and interactions. The set of highly altered genes (seed and linked genes) obtained through network analysis was then subjected to function and interaction analysis (Figure 4.7). For gene set enrichment analysis (GSEA), we used ClueGO, a Cytoscape application to delineate gene ontology [Bindea, Mlecnik *et al.*, 2009], and differentiate genes with respect to their functional association with the biological processes and molecular reactome. Here, the nodes represent gene functions and edges represent interactions. Figure 4.8a shows most enriched biological processes associated with the highly altered gene set. Similarly, complete reactome associated with the altered gene set and their interactions is shown in figure 4.8b. The gene enrichment analysis provided a comprehensive view and understanding of highly altered genes, their functions, interactions and associated-genomic pathways and interactions.

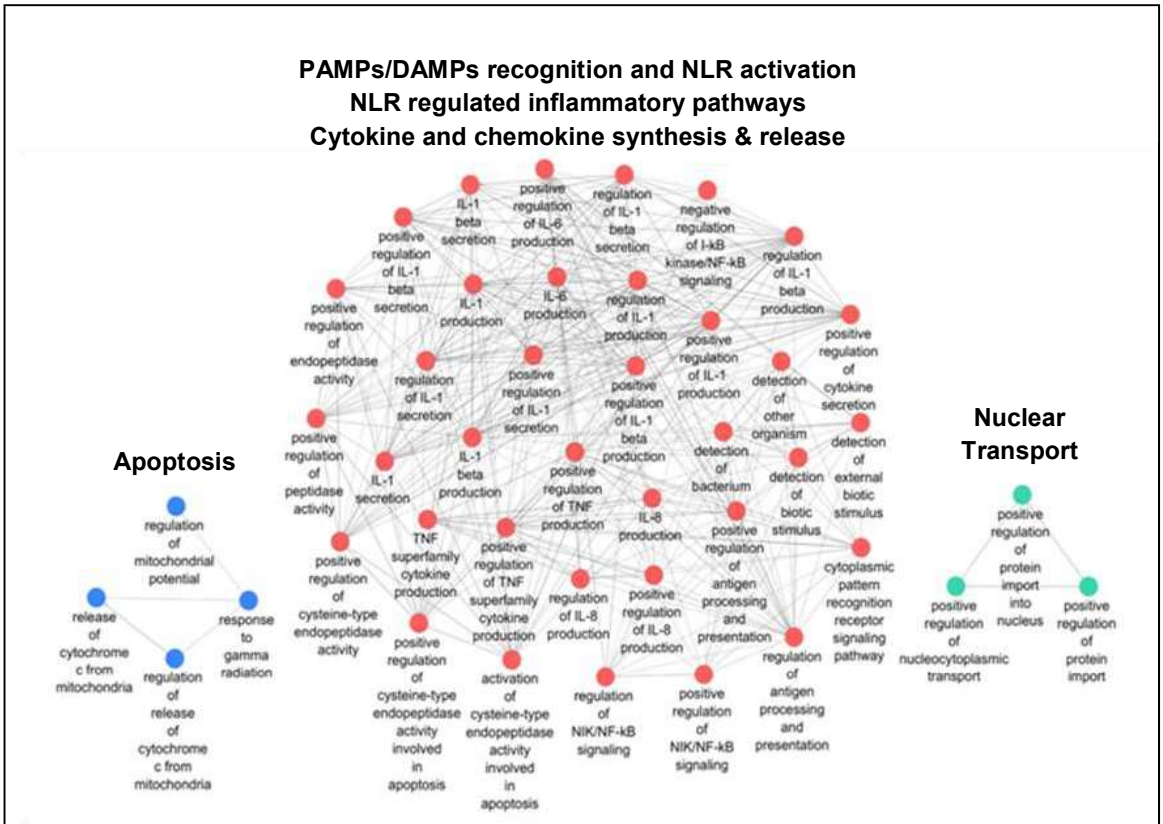

Figure 4.7 : *Gene ontology (GO) analysis of significantly altered genes and associated biological processes.* GO analysis performed for the network genes with respect to their association with biological processes. Here, each node represents a biological process for enriched set of genes. The edges represent different interaction types between genes involved in two biological processes. Genes have been categorized functionally into apoptosis, nuclear transport and NLR-regulated pathways including PAMPs/DAMPs recognition, inflammasome activation, cytokines & chemokine transcription and release, and major inflammatory pathways.

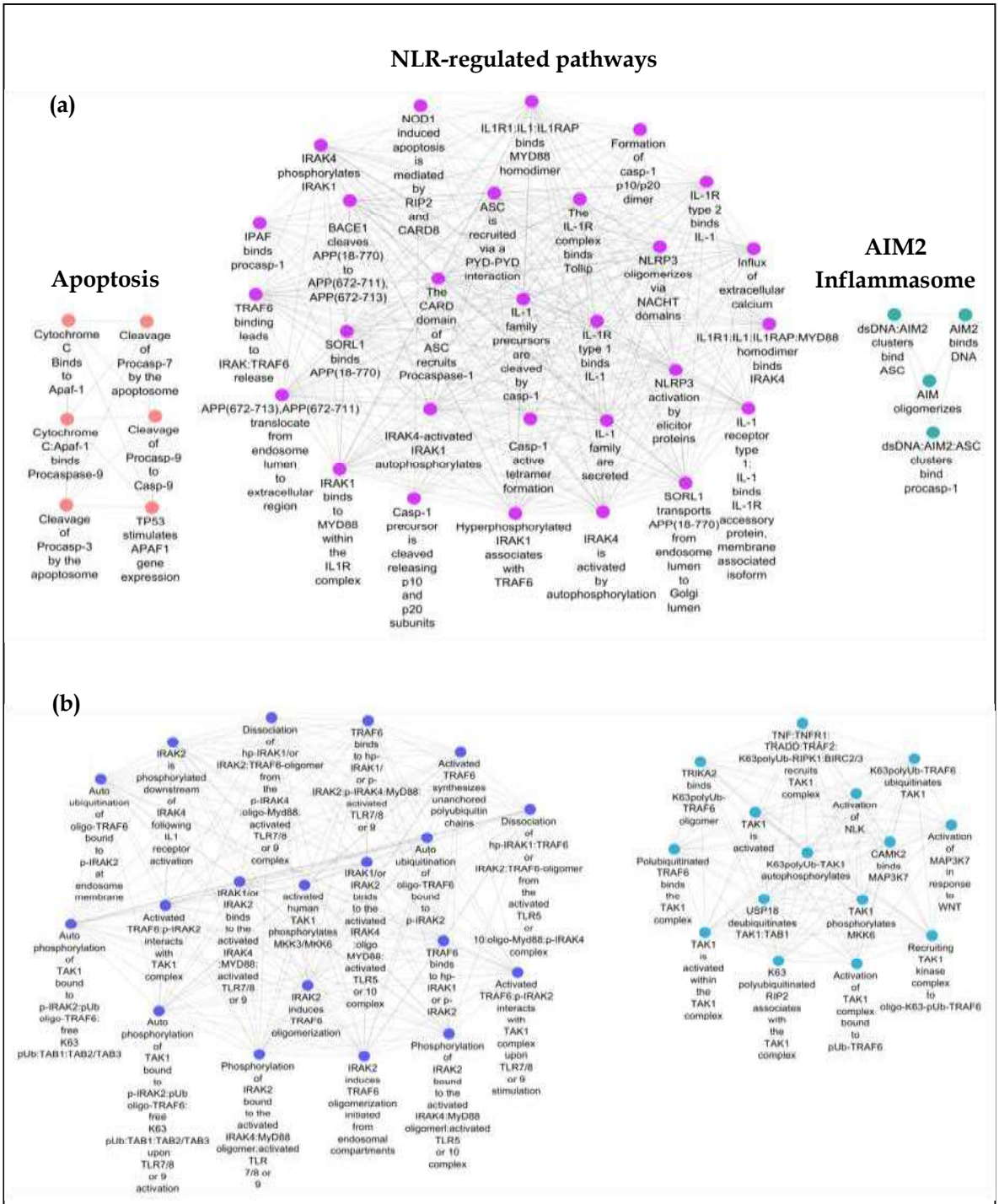

Figure 4.8: *Gene set enrichment analysis (GSEA) delineates gene ontology (GO) of significantly altered genes and their interactions within the biological reactome.* (a, b) GSEA provides comprehensive view of all biological processes associated with the seed and linked genes. Each node here represents an interaction for an enriched set of genes. The edges represent different interactions occurring within the pathways. The GSEA results have been divided into figure (a) and (b) for simplicity.

4.4.6 Prognostic value of NLRs and NLR-associated genes in glioma

Identification of gene signature, comprising of genes associated with different cellular components, functions and pathways to predict behavior of heterogeneous GBM tumors is of high research interest. The microarray-based gene expression profiling helped us in identification of the differentially expressed genes and their association with the early prognosis and clinical outcome of GBM patients. We investigated whether the elevated expression of NLRs and other network genes was related to the prognosis of patients with glioma. Differentially expressed NLRs and other-associated genes were evaluated for understanding their clinical importance using Kaplan-Meier survival curve analysis. For survival analysis, we calculated correlation of differentially expressed genes with patient's survival, using the survival R package. To evaluate the biomarker in several conditions, the dataset was chosen to reflect patients suitable for the test. Hence, we selected relevant TCGA LGG (grade 2 & 3) and GBM (grade 4) glioma patient samples and corresponding clinical information of TCGA RNA-seq gene expression data (pan-can normalized). We used Kaplan-Meier method to assess the prognostic value of the corresponding gene in different grades of glioma. We performed the analysis based on gene expression profiles and stratified patients based on mortality (Figure 4.9). To understand dysregulation of NLRs during both LGG and GBM, we considered the grade 2 and grade 3 (LGG) as first and second category, and grade 4 (GBM) in third category.

Patient samples were divided into two categories based on the median expression value of the corresponding gene. For grade 2 category of LGG, patients (n = 225) defined by high expression values for the gene of interest were grouped into high-expression group (black colored curve) and remaining are grouped into low-expression group (red colored curve). Similarly, for grade 3 category of LGG, patients (n = 248) having high expression values for the gene of interest were grouped into high-expression group (black colored curve) and remaining are grouped into low-expression group (red colored curve). For GBM, most aggressive grade of glioma category (Grade 4), the patients (n = 156) having high expression values for the specific gene were grouped into high-expression group (black colored curve) and remaining were grouped into low-expression group (red colored curve). For all the survival curve analysis, p-value <0.05 was considered significant. From the figure 4.9 (grade 2), it is clear that *BCL10* (P<0.04), *BCL2L1* (P<0.009), *CARD8* (P<0.009), *CDK11B* (P<0.009), *MSR1* (P<0.02), *NLRP6* (P<0.03), *NOD1* (P<0.03) and *PYCARD* (P<0.01) genes significantly separates the two risk groups characterized by differences in their gene expression with p-value of log-rank test. From the survival curves, it is seen that higher expression of these genes leads to poor overall survival of the glioma patients. We also identified *ATN1* (P<0.0008), *CASP1* (P<0.005), *EGFR* (P<0.04), *MSR1* (P<0.05), *NLRC4* (P<0.04) and *TP53* (P<0.04) genes, contributing significantly to low overall survival rate of the grade 3 glioma patients (Figure 4.10(a)). *EGFR*, *TP53* and other important genes with high genomic alterations in glioma networks and significant differential expression across different grades of glioma, did not show any prognostic value for grade 4, GBM patients. Differentially expressed genes showing significant association with overall survival, emerge as promising biomarkers for prognostically significant molecular sub-typing of low and high grade glioma. Interestingly, for GBM, *NLRP12* significantly separates the two risk groups characterized by differences in their gene expression with p-value of log-rank test of 0.03 (Figure 4.10(b)). Based on its high significance level, we suggest *NLRP12* as a possible prognostic marker for GBM.

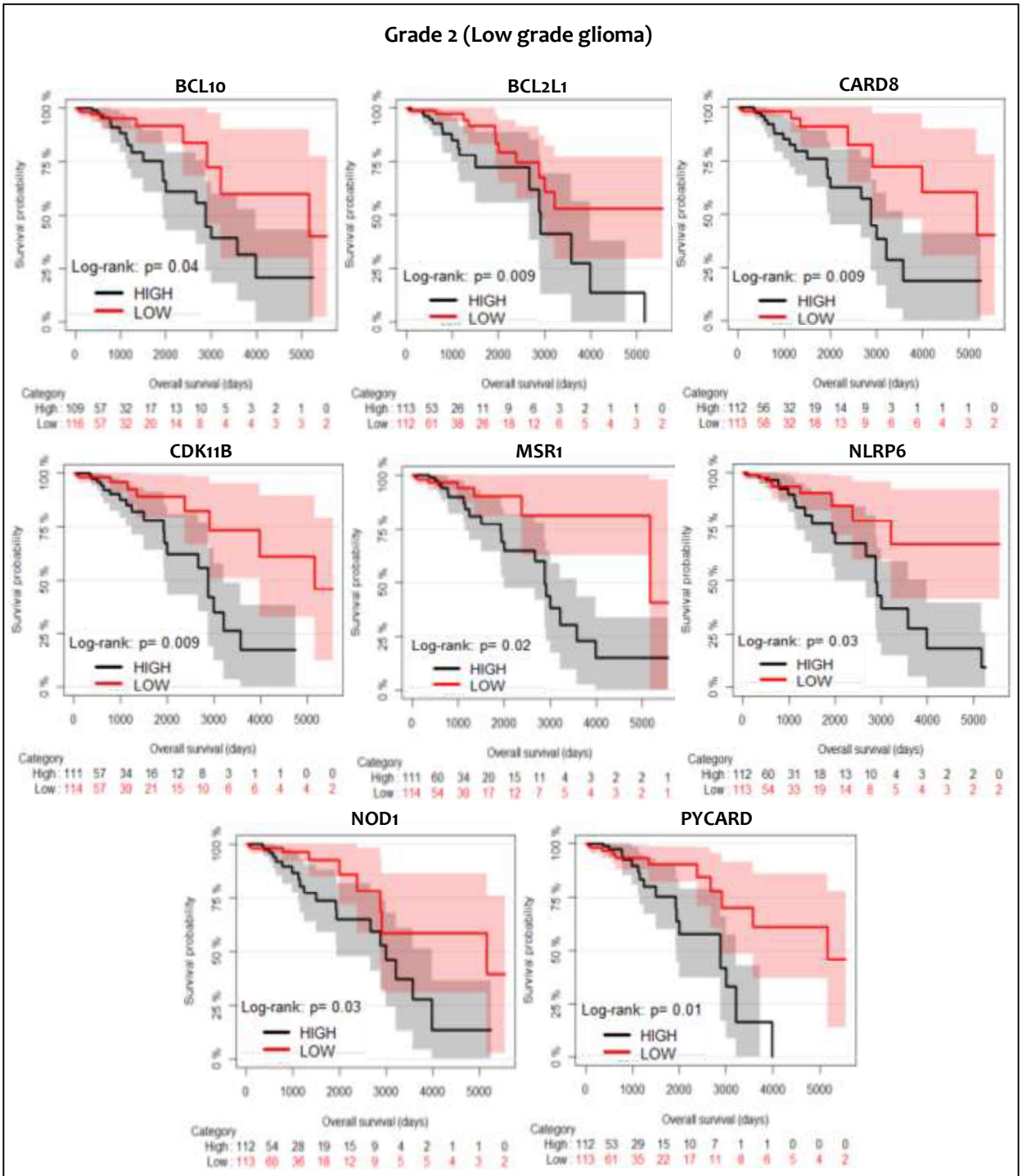

Figure 3.9: *Kaplan-Meier (KM) survival curves of TCGA LGG (grade 2) stratified by the expression of NLRs.* The KM curves show significant association of NLRs and other related genes with the patient survival outcome. The black and red curves indicate high and low gene expression respectively. The p values from log-rank tests comparing the two KM curves are mentioned for each figure.

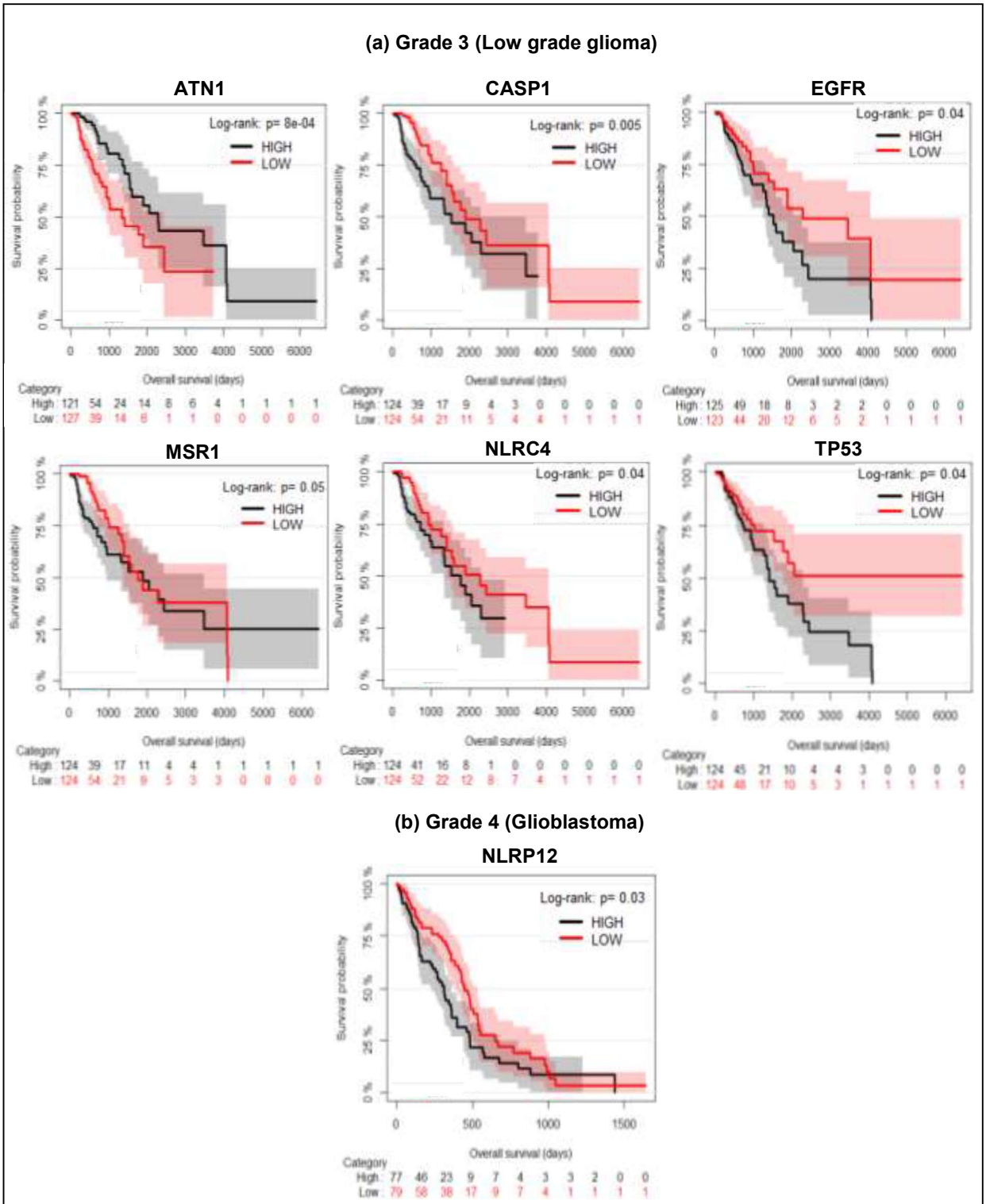

Figure 4.10 : *Kaplan-Meier (KM) survival curves of TCGA LGG and GBM patients stratified by the expression levels of NLRs.* (a, b) shows the survival curve for genes having significant association with the glioma survival outcome in the LGG (grade 3) and GBM (grade 4) patient samples. The p values from log-rank tests comparing the two KM curves are mentioned for each figure.

4.4.7 Kaplan-Meier survival analysis for TCGA LGG and GBM using REMBRANDT platform

To gain more confidence from our analyses and results, we assessed previously identified differentially expressed genes for glioma using an additional glioma database platform, REMBRANDT. The impact of *CARD8*, *CASP1*, *MSR1, PYCARD* and *PARP1* gene expression on overall survival was found to be statistically significant for LGG patient datasets (Figure 4.11). The results obtained for association between differentially expressed genes and overall survival using the REMBRANDT glioma dataset, were quite similar to the TCGA glioma datasets. Comparative analysis across two data platforms and similarity within the findings supports the selection of above identified genes as important prognostic biomarkers for different grades of glioma.

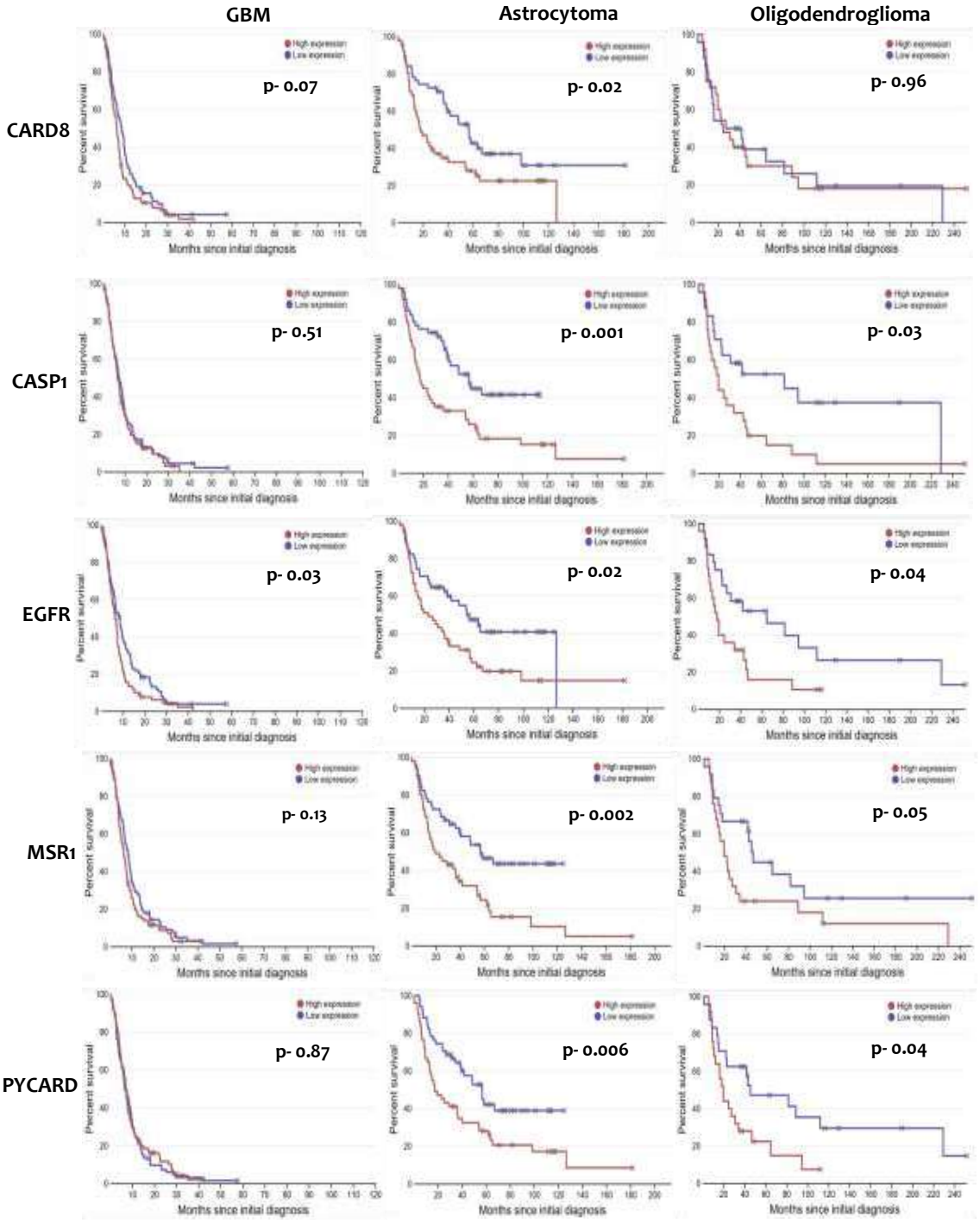

Figure 4.11 : *Kaplan-Meier (KM) survival curves for GBM and LGG stratified by the expression of NLRs and NLR-associated genes using REMBRANDT.* Here, LGG has been divided into two categories – astrocytoma and oligodendroglioma. Figure shows *CARD8, CASP1, EGFR, MSR1 and PYCARD* genes having significant association with the glioma survival outcome. The P values from log-rank tests comparing the two KM curves are mentioned for each figure.

4.4.8 Kaplan-Meier survival analysis for differentially expressed genes in other TCGA cancer types

To confirm, if the above identified genes association with patient survival is specific to LGG and GBM, we did similar survival curve analysis on other TCGA cancer datasets- Colon adenocarcinoma (COAD), Lung adenocarcinoma (LUAD) and, Head and neck squamous cell carcinoma (HNSC) (Table 4.3). However, we did not find any significant association between differentially expressed GBM genes and patient survival for all the three cancer types. The pan-cancer survival analysis further confirms that the differential expression and methylation, as well as the clinical relevance of NLRs and other associated genes, is specific to LGG and GBM.

Table 4.3: *P-values for Kaplan-Meier survival curve analysis of multiple TCGA cancer datasets*

Gene	P-values of Log Rank Test (Kaplan-Meier survival curve)		
	Colon Adenocarcinoma	Lung Adenocarcinoma	Head and Neck Squamous Carcinoma
NOD1	0.2	0.4	0.6
PYCARD	0.7	0.5	0.8
CARD8	0.4	0.1	0.1
NLRP12	1	0.5	0.5
CASP1	0.4	0.4	0.2
BCL2L1	***0.01**	1	0.8
ATN1	0.7	1	0.1
NLRC4	0.1	0.4	0.6
EGFR	0.9	0.6	***0.04**
BCL10	0.08	0.4	***0.04**
TP53	0.6	0.9	1
PARP1	0.1	0.8	0.3
CDK11B	0.4	0.6	0.6
NLRP6	0.5	0.5	0.06
MSR1	0.9	0.5	0.3

*KM survival curves of pan-cancer TCGA data analysis for colon adenocarcinoma, lung adenocarcinoma and, head and neck squamous cell carcinoma patients. The expression data was stratified by the expression levels of NLRs and NLR-associated genes. Level of significance: P-value <0.05 (log - rank test).

4.4.9 NLRs and NLR-associated gene expression in normal and glioma cell population using immunofluorescence.

TCGA database provides a comprehensive genome profiling of patients with different cancer types. The data comes from multiple medical sources and platforms contributed to the TCGA data portal, and gathered from analysis performed using the whole tumor/normal tissue. The multi-platform data collection and analyses, neglects individual tissue or cell population effects. Growing evidences suggest cell and tissue-specific roles of NLRs in cancer [Hu, Elinav *et al.*, 2010; Chen, Liu *et al.*, 2011]. Therefore, to better understand the cellular profiling of NLRs contributing to the glioma tumor microenvironment, we looked at the expression of differentially expressed NLRs and NLR-associated genes, namely *ASC /PYCARD*, *AIM2* and *CASP1* in multiple innate immune and glioma cell population. We have used A172 and LN-18, human GBM-derived cell lines as *in-vitro* glioblastoma study models. Additionally, we have used RAW264.7 macrophages,

Human umbilical vein endothelial cells (HUVECs), N9 and BV2 microglial cells, and C6, rat glioma cells as control.

We have identified cellular expression of *ASC*, *AIM2* and *CASP1* at the protein level under normal and inflammatory (LPS-primed) conditions using immunofluorescence (Figure 4.12-4.17). We observed significantly higher intensity/expression of *NLRP12, AIM2* and *CASP1* genes in microglia and human GBM cell lines. The high expression levels suggest intact gene regulation of NLRs and associated mediators during glioma pathogenesis.

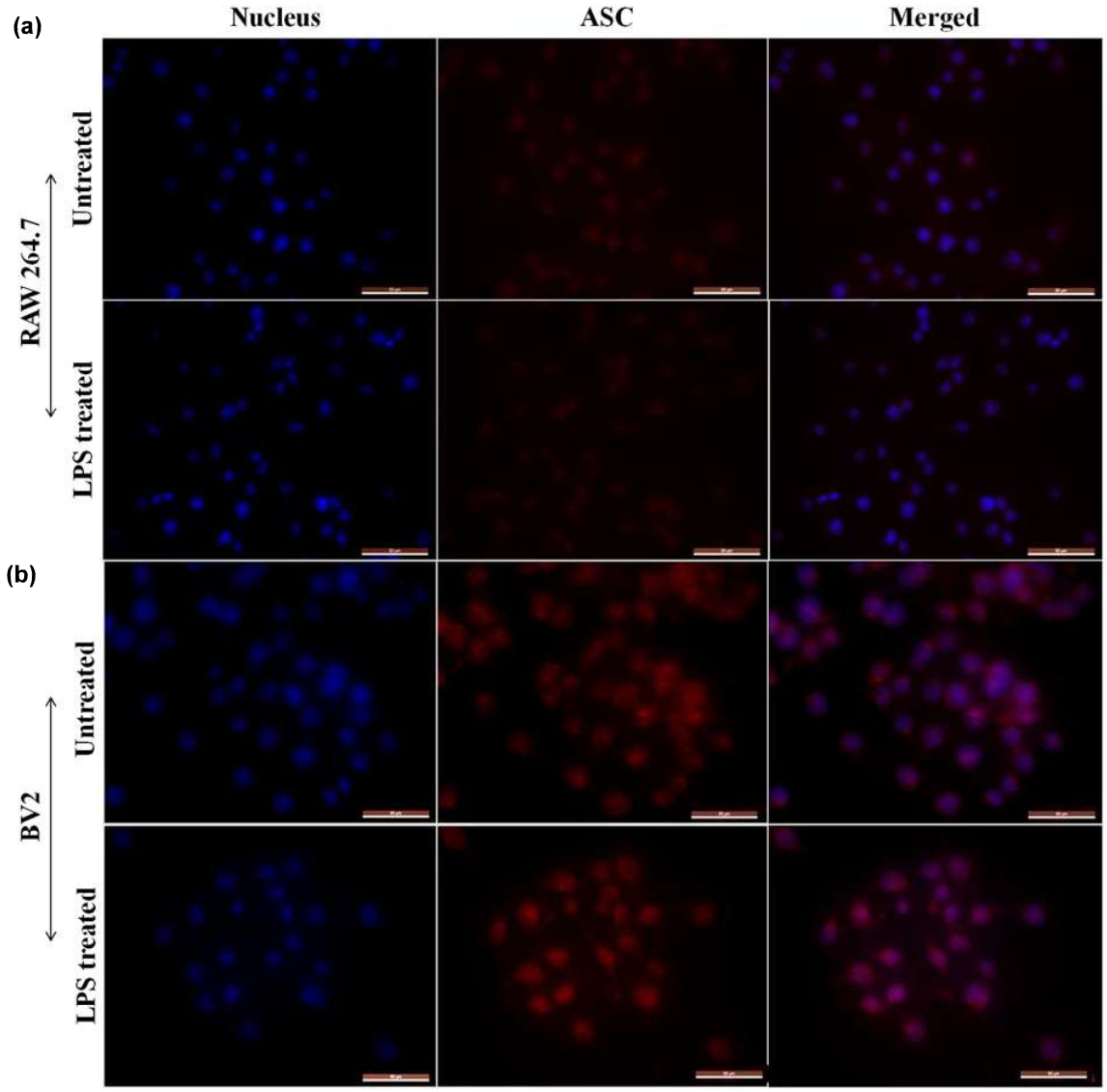

Figure 3.12 : *Immunocytochemistry for ASC protein expression in microglia and macrophages.* (a, b) Above panel shows ASC / PYCARD protein visualization in untreated and lipopolysaccharide cell lines. Scale bar: 50µm.

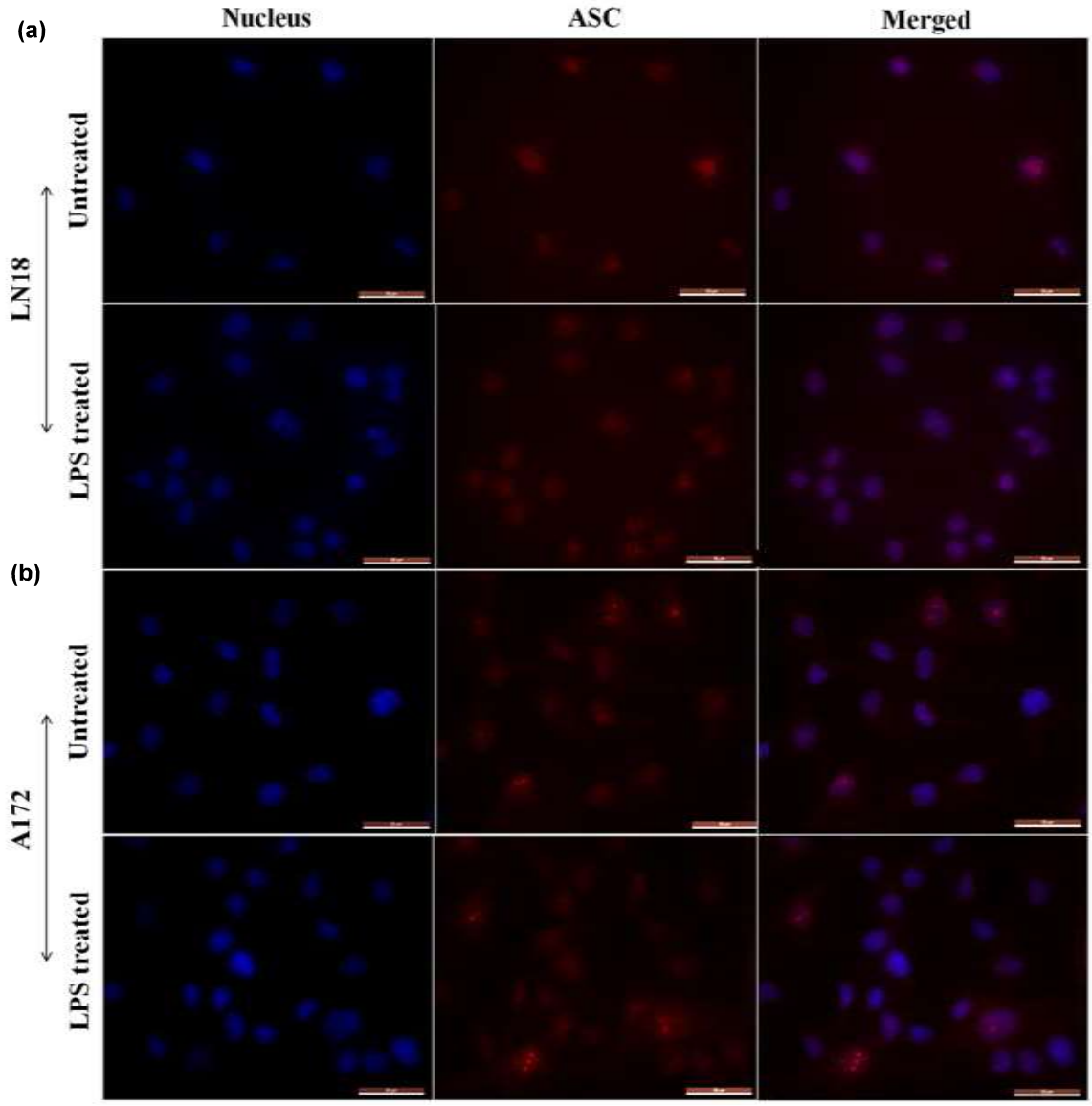

Figure 4.13 : *Immunocytochemistry for ASC protein expression in gliomas.* (a, b) Above panel shows ASC protein visualization in untreated and LPS-primed LN-18 and A172 glioma cell lines. Scale bar: 50µm. Nuclei are stained blue with DAPI. Insets show antibody control.

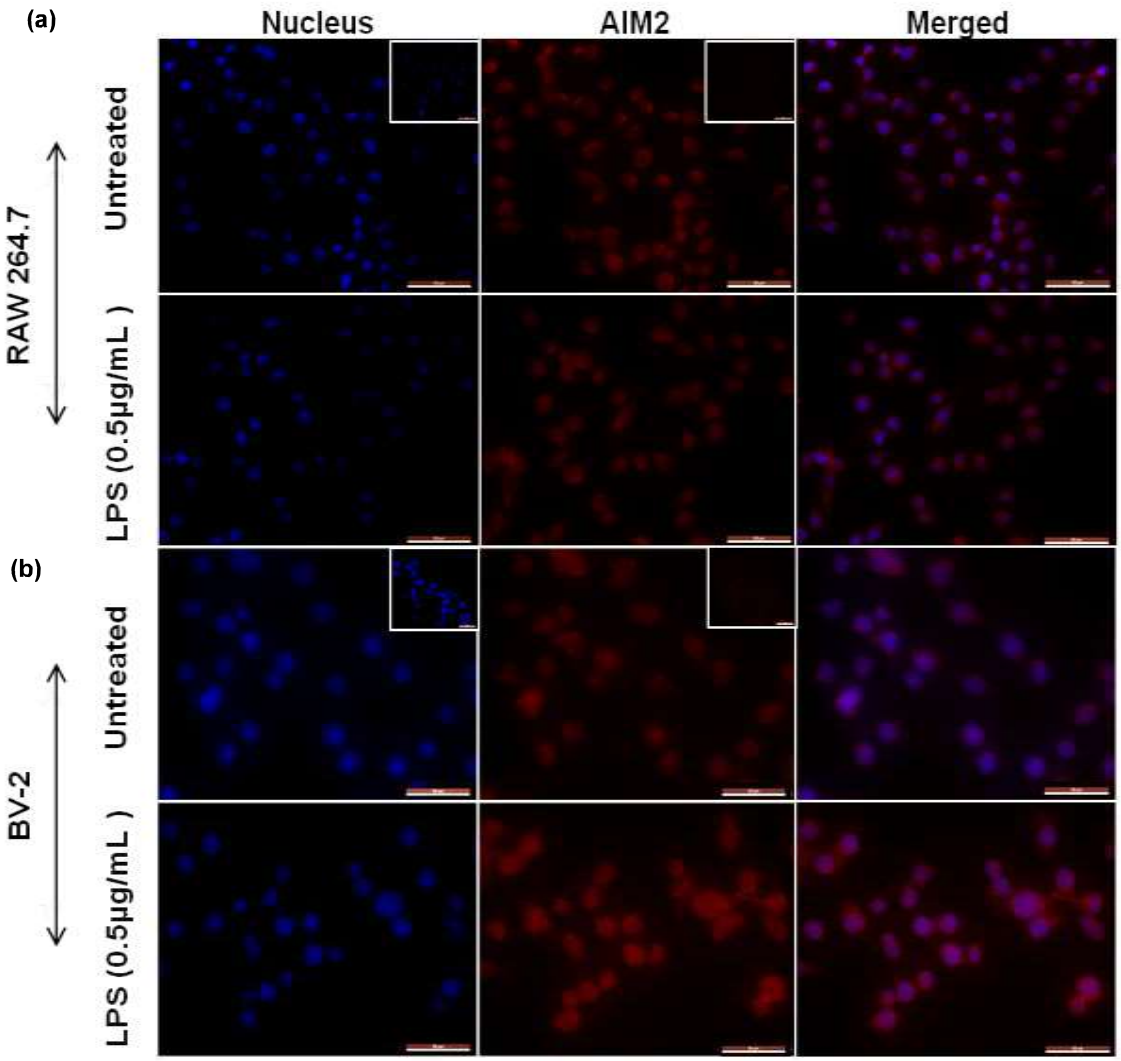

Figure 4.14 : *Immunocytochemistry for AIM2 protein expression in microglia and macrophages.* (a,b) Above panel shows AIM2 protein visualization in untreated and LPS-primed RAW macrophages and BV-2 microglia cell lines. Scale bar, 50µm (a,b). Nuclei are stained blue with DAPI. Inset shows antibody control.

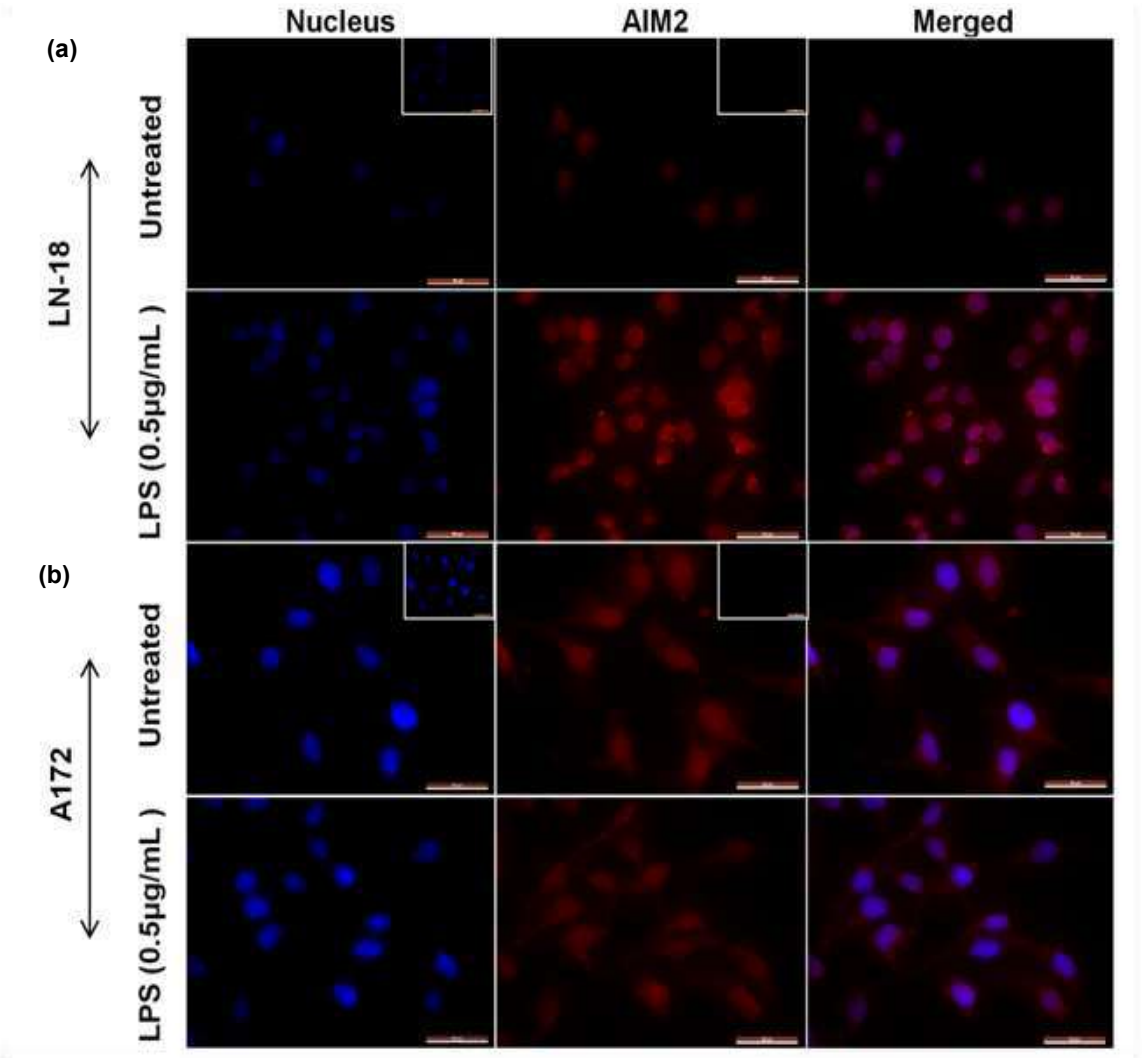

Figure 4.15 : *Immunocytochemistry for AIM2 protein expression in gliomas.* (a,b) Above panel shows AIM2 protein visualization in untreated and LPS-primed LN-18 and A172 glioma cell lines. Scale bar, 50µm (a,b). Nuclei are stained blue with DAPI. Inset shows antibody control.

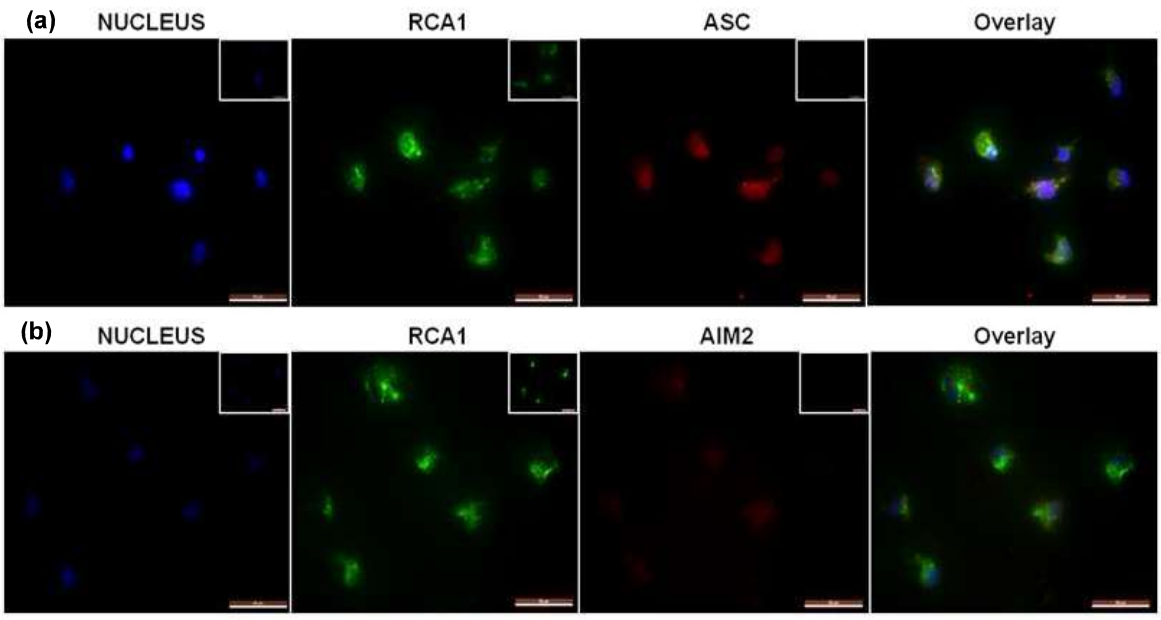

Figure 4.16 : *Immunocytochemistry for ASC and AIM2 protein expression in primary endothelial cells.* (a,b) Above panel shows ASC and AIM2 protein expression in RCA1 stained endothelial cells (HUVECs). Scale bar, 50µm . Nuclei are stained blue with DAPI. Inset shows antibody control.

*****

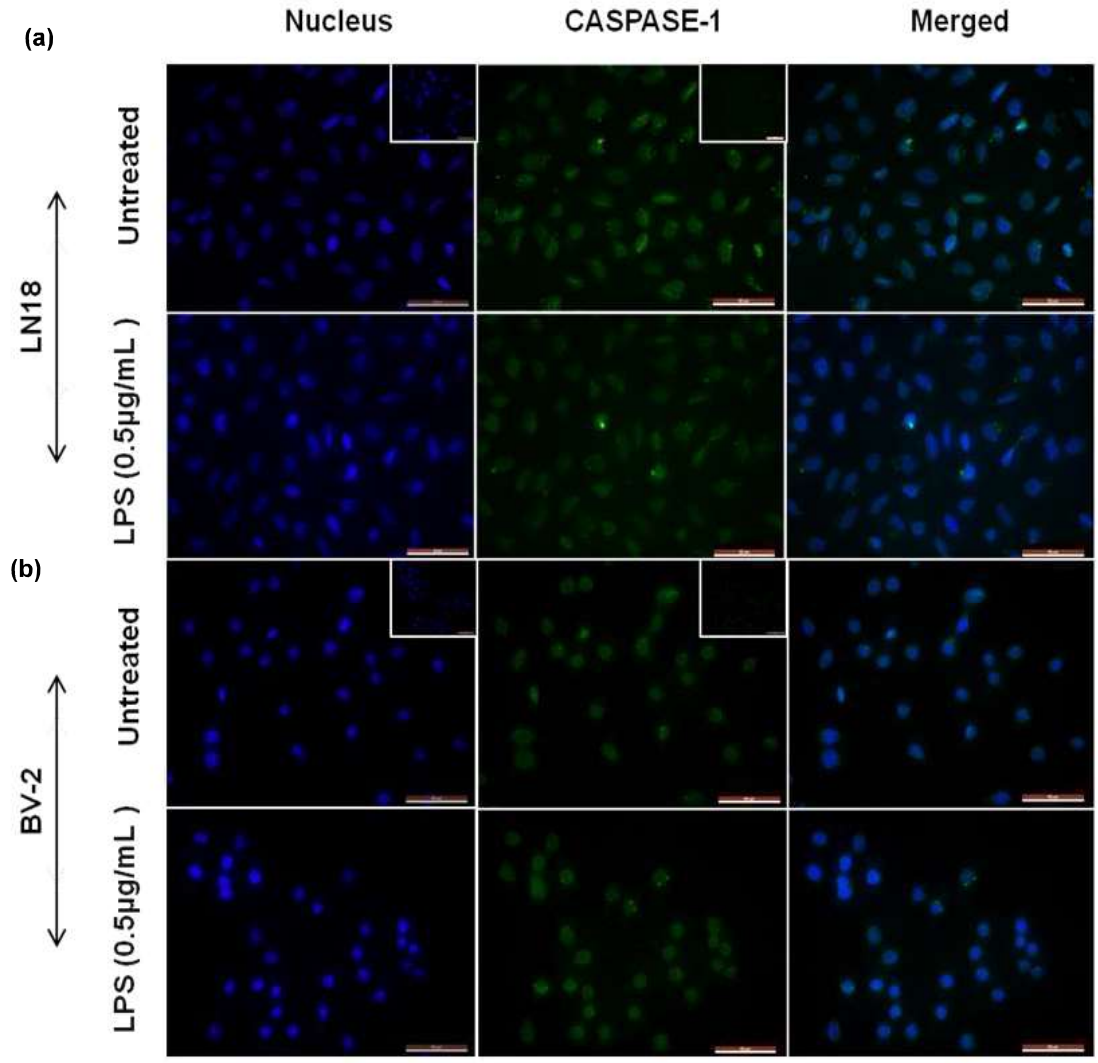

Figure 4.17 : *Immunocytochemistry for Caspase-1 protein expression in glioma and microglial cells.* (a,b) Above panel shows Caspase-1 (CASP-1) expression in untreated and LPS-primed LN-18, human glioma and BV-2, microglial cell lines. Scale bar, 50µm (a,b). Nuclei are stained blue with DAPI. Inset shows antibody control.

4.4.10 NLRP12 regulates cellular proliferation in glioblastoma

The *NLRP12* gene regulates non-inflammasome and anti-inflammatory signaling by inhibiting both canonical and non-canonical NF-κB pathways [Zaki, Man *et al.*, 2013; Chen, 2014]. *NLRP12* performs negative regulation of non-canonical NF-κB to suppress colon inflammation and tumor formation in experimental colitis-induced mice [Allen, Wilson *et al.*, 2012]. Recently, NLRP12 inflammasome-induced IL-1β and IL-18 signaling has been linked to host resistance against specific pathogens such as *Yersinia pestis* [Vladimer, Weng *et al.*, 2012]. From the TCGA glioma findings, we show significant differential gene expression and methylation of *NLRP12* in GBM with respect to LGG. We found significantly high negative correlation between the *NLRP12* expression and methylation levels for GBM. In survival curve analysis, *NLRP12* showed high prognostic value for GBM, which motivated us to examine the expression and functional association of *NLRP12* with glioma, using microglial (BV2 and N9) and GBM (LN18) cell lines.

Using immunofluorescence, we were able to characterize high NLRP12 expression in untreated and LPS-primed BV2 (Figure 4.19a), LN18 and N9 cells (Figure 4.18 (a, b)). To understand the role of NLRP12 in glioma cell proliferation, we utilized *NLRP12*si RNA and performed colony formation assay on microglial cells. The bright-field image analysis of Giemsa-stained microglial cells shows the increase in colony formation upon *NLRP12* inhibition (Figure 4.19b). The results were quantifed for each sample, by counting the number of colonies formed per well and number of cells present per colony. As observed, *NLRP12* inhibition leads to an increased number of cell colonies (Figure 4.19c). Based on current findings, we suggest *NLRP12* inhibition leads to increased cellular proliferation *in vitro*. However, further experimental analysis needs to be done, to confirm these preliminary findings and determine other functions and pathways associated with *NLRP12* gene in GBM.

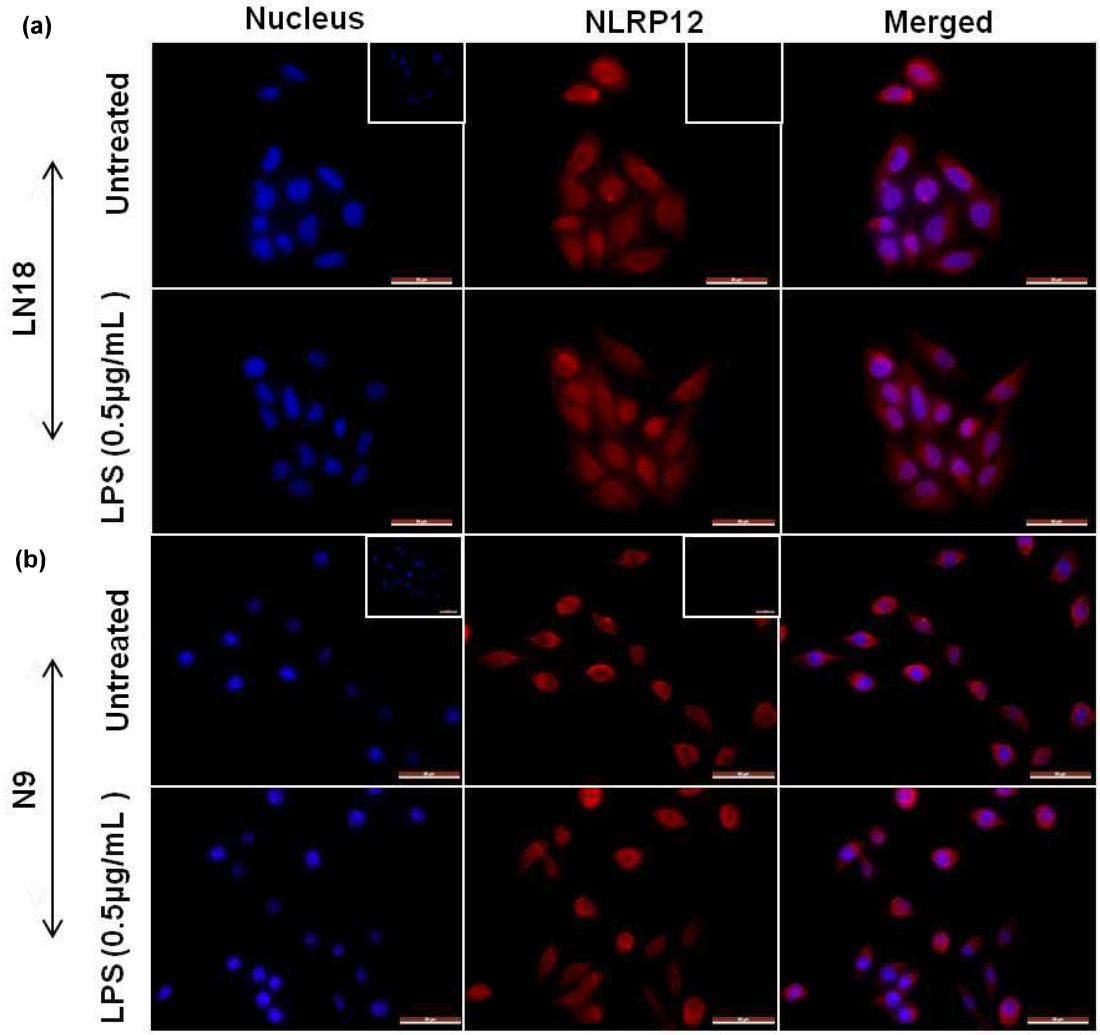

Figure 4.18 : *Immunocytochemistry for NLRP12 protein expression in glioma and microglial cells.* (a, b) Panel shows NLRP12 protein visualization in untreated and LPS-primed LN-18, glioblastoma and N9, microglial cells. Scale bar: 50µm. Nuclei are stained blue with DAPI. Inset shows antibody control.

[

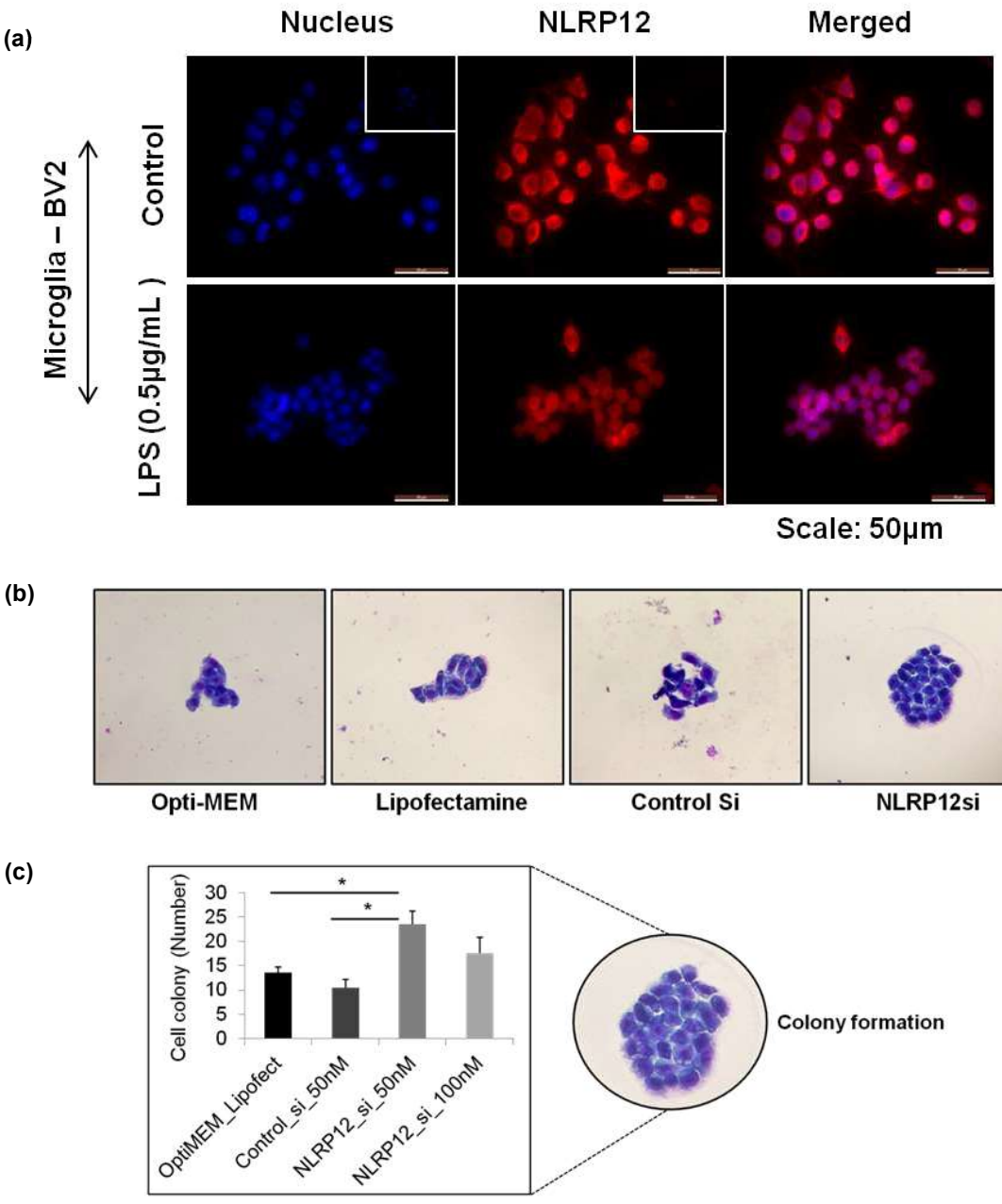

Figure 4.19 : *NLRP12 inhibition increases cellular proliferation in vitro.* (a) NLRP12 expression was observed in microglial cells using immunofluorescence. (b) Colony formation assay (CFA) was performed to visualize the effect of NLRP12 gene inhibition. Bright-field images indicate increased cellular proliferation in the NLRP12 siRNA treated microglia. (c) CFA results were quantified by counting cells per colony as well as the number of colonies formed for each of the sample. BF images were captured at 40X magnification, using a cell phone camera.

4.4 CONCLUDING REMARKS

Gliomas are the most aggressive type of primary brain tumors with poor prognosis and high mortality. Glioma tissue microenvironment is heavily infiltrated by the innate immune cells. The cellular and molecular interplay between the immune cells and glioma tissue forms the highly enriched tumor niche. NLRs are highly conserved cytoplasmic sensors regulating innate immunity, inflammation and inflammation-induced tumorigenensis. Despite their dual tumor-promoting and -inhibitory roles, the functional significance of NLRs in glioma remain unexplored. Our study utilized a multimodal data-driven approach to characterize the expression of NLRs and NLR-associated genes for low grade glioma and glioblastoma. We found significant differential methylation and expression of NLRs and other important genes associated with inflammation, cell death and DNA repair mechanisms in glioblastoma. Strong inverse correlation between expression and methylation levels of NLRs was found in GBM with respect to the LGG. NLRs and other associated genes showed significantly high coorelation with patient survival, in low and high grade glioma, reflecting their promising therapeutic significance. Notably, cell and tissue-specific roles of NLRs has been reported in cancer. Therefore, we characterized the expression of NLRs in innate immune and glioma cell population using different cell lines. Based on our TCGA – Glioma findings, we characterized the expression of NLRP12 in glioma cell population. Interestingly, we found NLRP12 as negative regulator of cellular proliferation *in vitro*. Current research provides novel insights into the differential regulation of NLRs and NLR-associated genes in LGG and GBM, and the prognostic importance of NLRs such as *NLRP12* and other *NLRs*-mediated innate immune signaling pathways in glioma pathology.